NASA TECHNICAL REPORT

ANALYSIS OF TRANSONIC FLOW ABOUT LIFTING WING-BODY CONFIGURATIONS

Richard W. Barnwell

Langley Research Center
Hampton, Va. 23665

NATIONAL AERONAUTICS AND SPACE ADMINISTRATION • WASHINGTON, D. C. • JUNE 1975

1. Report No.	2. Government Accession No.	3. Recipient's Catalog No.
NASA TR R-440		

4. Title and Subtitle	5. Report Date
ANALYSIS OF TRANSONIC FLOW ABOUT LIFTING WING-BODY CONFIGURATIONS	June 1975
	6. Performing Organization Code
7. Author(s)	8. Performing Organization Report No.
Richard W. Barnwell	L-9969
	10. Work Unit No.
9. Performing Organization Name and Address	505-06-11-02
NASA Langley Research Center Hampton, Va. 23665	11. Contract or Grant No.
	13. Type of Report and Period Covered
12. Sponsoring Agency Name and Address	Technical Report
National Aeronautics and Space Administration Washington, D.C. 20546	14. Sponsoring Agency Code

15. Supplementary Notes

16. Abstract

An analytical solution is obtained for the perturbation velocity potential for transonic flow about lifting wing-body configurations with order-one span-length ratios and small reduced-span-length ratios and equivalent-thickness-length ratios. The analysis is performed with the method of matched asymptotic expansions. The angles of attack which are considered are small but are large enough to insure that the effects of lift in the region far from the configuration are either dominant or comparable with the effects of thickness. The modification to the equivalence rule which accounts for these lift effects is determined. An analysis of transonic flow about lifting wings with large aspect ratios is also presented.

17. Key Words (Suggested by Author(s))	18. Distribution Statement
Transonic flow Lifting configurations Area rule Analytical solution	Unclassified – Unlimited New Subject Category 02

19. Security Classif. (of this report)	20. Security Classif. (of this page)	21. No. of Pages	22. Price*
Unclassified	Unclassified	73	$4.25

*For sale by the National Technical Information Service, Springfield, Virginia 22151

CONTENTS

ANALYSIS OF TRANSONIC FLOW ABOUT LIFTING WING-BODY CONFIGURATIONS

Richard W. Barnwell
Langley Research Center

SUMMARY

An analytical solution is obtained for the perturbation velocity potential for transonic flow about lifting wing-body configurations with order-one span-length ratios and small reduced-span-length ratios and equivalent-thickness-length ratios. The analysis is performed with the method of matched asymptotic expansions. The angles of attack which are considered are small but are large enough to insure that the effects of lift in the region far from the configuration are either dominant or comparable with the effects of thickness. The modification to the equivalence rule which accounts for these lift effects is determined. An analysis of transonic flow about lifting wings with large aspect ratios is also presented.

INTRODUCTION

It is well known that the outer part of transonic flow fields about lifting configurations at small angles of attack is governed largely by the effects of thickness. It has been shown by Oswatitsch and Keune (ref. 1) that the flow in the region far from nonlifting wing-body configurations is mathematically equivalent to that about axisymmetric bodies with the same cross-sectional area distributions. Whitcomb (ref. 2) has demonstrated experimentally that the wave drags of wing-body combinations at zero angle of attack are the same as those of the equivalent axisymmetric bodies. The analysis of Heaslet and Spreiter (ref. 3) shows that these zero-angle-of-attack results also apply to configurations at angles of attack of the order of the wing thickness or less. The main purpose of this report is to present an analytical solution for transonic flow about lifting configurations at angles of attack large enough to insure that the effects of lift either dominate or are comparable with the effects of thickness in the outer region.

The present problem and two similar problems which have been analyzed previously are compared in figure 1. The problem of transonic flow past slender bodies at angles of attack of the order of the equivalent-thickness-length ratio has been treated by Messiter (ref. 4), Hayes (ref. 5), and Lifshits (ref. 6) with the method of asymptotic expansions. The problem of transonic flow past wing-body combinations with spans of order one at

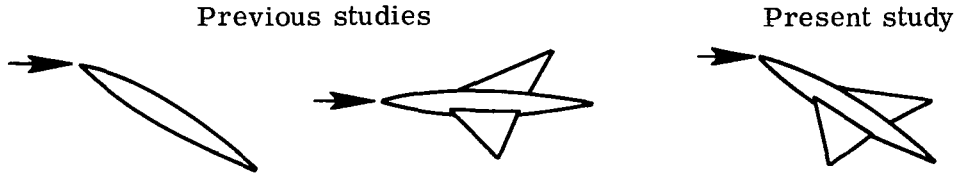

Figure 1.- Comparison of past and present transonic studies.

angles of attack proportional to the wing thickness-length ratio or smaller has been studied by Hayes (ref. 5) and by Cheng and Hafez (ref. 7) with the method of matched asymptotic expansions and by Heaslet and Spreiter (ref. 3) with the integral equation formulation. Since the flow is thickness dominated for both of these problems, the equivalence rule of Oswatitsch and Keune applies. As is indicated in figure 1, the present problem involves flow about wing-body combinations at angles of attack which are small but much larger than the wing thickness. In the first attempt at solving the present problem, Cheng and Hafez (ref. 7) obtained results which indicated that when the effects of lift and thickness were comparable in the outer region, the expressions for each of these effects are the same as that obtained when the effects of thickness are dominant. In the preliminary version of the present treatment (ref. 8), it was shown that, to the contrary, when the effects of lift and thickness are comparable in the outer region, there is a source flow due to lift which is of the same order of magnitude as the source flow due to thickness. Later in this paper, it is argued on physical grounds that this type of influence by lift is reasonable. As a result of the source flow due to lift, the equivalence rule of Oswatitsch and Keune is not applicable to the present problem. It should be noted that the radial length scale in the outer region obtained in reference 8 for the present problem was different from that obtained for the thickness-dominated problem. This difference in radial length scale resulted from the choice of relationship between the angle of attack and the equivalent thickness ratio which was used. In reference 9 Cheng and Hafez show that there is a second relationship between the angle of attack and the equivalent thickness ratio which leads to the same source flow due to lift obtained in reference 8 and which yields the same outer-region radial length scale found for thickness-dominated flows. This second length scale is physically more realistic and thus is the one used in this report.

In this report the analytical solution for transonic flow about lifting configurations with span-length ratio of order one and small reduced span-length ratios (the product of the span-length ratio and the factor $\sqrt{|1 - M_\infty^2|}$ when M_∞ is the free-stream Mach number) is derived in detail with the method of matched asymptotic expansions. This solution is determined to within an arbitrary additive function of the length along the axis which cannot be determined with the present method. There is a brief discussion of how this

function can be determined by use of numerical techniques. Also a study is made of the problem of lifting transonic flow about configurations with large aspect ratios.

SYMBOLS

$A(\tilde{x}),B(\tilde{x}),C(\tilde{x})$ arbitrary functions in unmatched outer expansion

$A_0(\tilde{x}),B_0(\tilde{x})$ functions in twist and camber potential (see appendix B)

a constant of proportionality in equation (54) for angle of attack

b wing semispan

C_p pressure coefficient

C_w constant of proportionality of order one (see eqs. (3) and (95))

c exponent, $0 \leq c \leq 1$

$\tilde{d}_v,\tilde{z}_v$ Cartesian coordinates locating vortex core relative to wing tip (see fig. 8)

E complete elliptic integral of second kind

$F(\tilde{x})$ nondimensional thickness distribution of body

$F_e(\tilde{x})$ nondimensional thickness distribution of equivalent body

$f(\tilde{x})$ nondimensional dipole strength distribution

$G_1(\tilde{x}),G_3(\tilde{x})$ arbitrary additive functions in outer expansion (see eq. (68))

$g(\tilde{x},\tilde{y})$ twist and camber distribution of wing

$g_n(\tilde{x}),g_{m,n}(\tilde{x})$ arbitrary additive functions in inner potentials ϕ_n and $\phi_{m,n}$

$g_\delta(\tilde{x})$ arbitrary additive function in inner thickness potential φ_δ

$H(\tilde{x})$ secondary source-strength distribution in outer expansion given by equation (51)

$h(\tilde{x},\tilde{y})$ thickness distribution of wing

K $= \frac{1 - M_\infty^2}{\epsilon_1}$; also complete elliptic integral of first kind

k modulus of E and K given by equation (26)

L characteristic length in x-direction

ℓ characteristic length in x-direction, configuration length unless otherwise noted

M_∞ free-stream Mach number

$m(\tilde{x},\tilde{y})$ $= \frac{1}{2}(m_+ - m_-)$

$m_+(\tilde{x},\tilde{y}), m_-(\tilde{x},\tilde{y})$ functions in equation (29) for potential ϕ_1 near configuration surface

N nonnegative number

q_x, q_r, q_θ body-oriented cylindrical polar velocity components (see eqs. (2))

r radial body-oriented coordinate

$r_b(x)$ radius of body surface

$S(\tilde{x})$ Mirels' S-function (also Mangler's H-function)

S_a' lowest order source strength of configuration in outer region (see eqs. (69), (70), and (71))

s distance in cross-flow plane along wing and leading-edge vortex sheet from center of wing

t maximum thickness of equivalent body

t_w maximum thickness of wing

U_∞ free-stream speed

u,v,w	body-oriented cylindrical polar perturbation velocity components
v_c,w_c	body-oriented Cartesian perturbation velocity components in y- and z-direction, respectively
W	complex potential
X	complex variable, $\tilde{y} + i\tilde{z}$
x,y,z	body-oriented Cartesian coordinates (see fig. 3)
Y	complex function defined by equation (A2)
$y_2(x),y_1(x)$	leading and trailing edges of wing
Z	transformed complex variable defined by equation (A16), $\eta + i\xi$
z_w	z-coordinate of wing surface
α	angle of attack
β	angle defined by equations (A9) or (A14)
Γ_v	strength of vortex core
γ	ratio of specific heats
$\gamma(\tilde{x},s)$	vortex strength of wing or vortex-sheet segment
$\Delta\phi$	potential jump across vortex-sheet segment
δ	equivalent body thickness ratio, t/ℓ
ϵ_n	nth gage function in outer expansion for φ
η,ξ	coordinates in transform planes (see figs. 8 and 9)
η_2,η_1	η-coordinates of leading and trailing edges of wing (see fig. 9)
θ	body-oriented polar angle (see fig. 3)

Λ $= \frac{b}{L}$

λ $= \frac{b}{\ell}$

μ_n nth gage function in intermediate expansion for φ

ν stretching parameter for outer radial coordinate

ρ infinitesimal radius

σ angle in transform plane depicted in figure 8

Φ_n nth potential in outer expansion for φ

$\phi_{m,n}$ potential in inner expansion for φ with gage function $\log_e^m\left(\frac{1}{\lambda\nu}\right)\sin^n\alpha$

ϕ_n potential in inner expansion for φ with gage function $\sin^n\alpha$

ϕ_{1a},ϕ_{1b} components of potential ϕ_1 (see appendix B)

$\phi_{2a},\phi_{2b},\phi_{2c},\phi_{2d}$ components of potential ϕ_2 (see appendix C)

φ perturbation velocity potential

$\varphi_\delta,\varphi_{\delta,1}$ thickness potentials in inner expansion for φ

χ_n nth potential in intermediate expansion for φ

ψ component of thickness potential φ_δ given by equation (30)

ω,ω_1,ω_2 angles shown in figure 10

∇_2^2 two-dimensional Laplace operator in cross-flow plane (see eqs. (12) and (21))

Superscripts:

C complementary solution

P particular solution

Subscripts:

max maximum value

v vortex

A bar over a symbol denotes outer variable (see eqs. (9)). A tilde over a symbol denotes inner variable (see eqs. (8)). A circumflex over a symbol denotes an intermediate variable (see eqs. (72)). Primes denote differentiation with respect to $\tilde{x}$, $\bar{x}$, or $\hat{x}$. An asterisk denotes a complex conjugate.

EFFECT OF LIFT AT NEAR-SONIC SPEEDS

It is well known that the effect of thickness is to deflect streamlines outward from the configuration. It can be shown that for near-sonic flow, lift can also have this effect in addition to the usual downwash effect. The manner in which lift causes the outward deflection of streamlines is depicted schematically in figure 2. The cross-sectional area

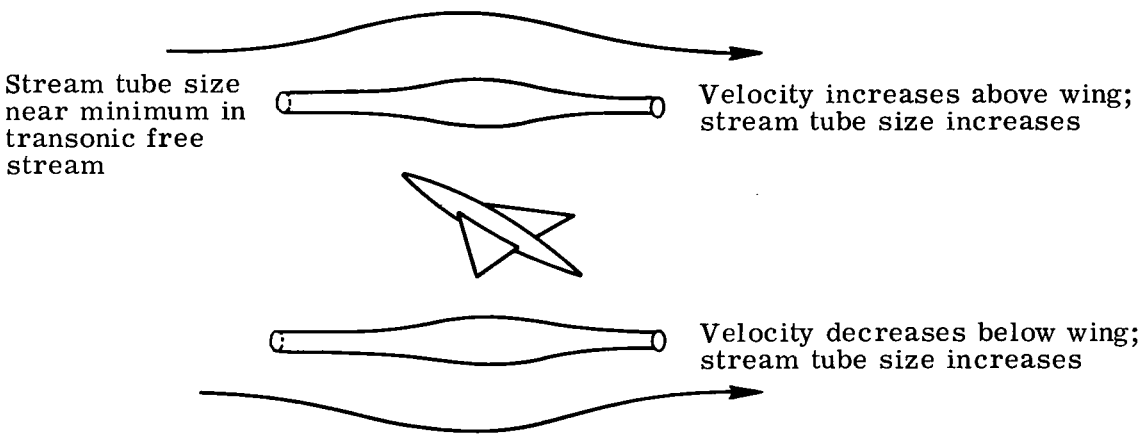

Figure 2.- Outward displacement of streamlines by both lift and thickness effects.

of stream tubes is minimum where the flow is sonic. The effect of lift is to increase the fluid speed in stream tubes above the wing and to decrease the speed in the tubes beneath the wing. For configurations traveling at Mach numbers near 1, both the increase and decrease in fluid speed are deviations from near-sonic flow. Thus for sufficiently large angles of attack, the cross sections of practically all the stream tubes about the body increase so that the streamlines are deflected outward more than they would be by thickness effects alone. The magnitude of the angle-of-attack range in which this phenomenon occurs will be established subsequently. It should be noted that the phenomenon does not

occur for completely subsonic or completely supersonic flow, where an increase in stream-tube size on one side of the wing is compensated by a decrease on the other.

SLENDER CONFIGURATION PROBLEM

Wings are described traditionally as being slender if the reduced span (the product of the span and the factor $\sqrt{|1 - M_\infty^2|}$) is much smaller than the length. In this section an analytical solution is obtained for transonic flow past slender configurations with span-length ratios of order one which are at angles of attack large enough to insure that the effects of lift and thickness are comparable at large distances from the configurations. The method of matched asymptotic expansions is used. The solution is determined to within an arbitrary additive function of distance along the axis which cannot be obtained with the present method. There is a brief discussion of methods which can be used to determine the additive function.

Problem Description

In this subsection the problem is described and the governing equation and boundary conditions are established. The problem is to analyze transonic flow about lifting wing-body configurations with small equivalent-thickness ratios δ and semispan-length ratios λ of order one which are at angles of attack α so that the effects of lift in the outer region either dominate or are comparable with the effects of thickness. Let the free-stream Mach number, the configuration length and semispan, and the maximum thicknesses of the wing and equivalent body be M_∞, ℓ, b, t_w, and t, respectively. The flow fields which are considered in this section are characterized by the parameters

$$\left.\begin{aligned} &|M_\infty - 1| \ll 1 \\ &\lambda = \frac{b}{\ell} = O(1) \\ &\delta = \frac{t}{\ell} \ll 1 \\ &\frac{t_w}{\ell} \ll 1 \\ &\alpha \ll 1 \end{aligned}\right\} \tag{1}$$

Body-oriented cylindrical polar and Cartesian coordinate systems are used in this report. These coordinate systems are shown in figure 3. For a vehicle at an angle of attack α, the total velocity components in the x-, r-, and θ-directions are

$$
\left.
\begin{aligned}
q_x(x,r,\theta) &= U_\infty \cos\alpha + u(x,r,\theta) \\
q_r(x,r,\theta) &= U_\infty \sin\alpha \sin\theta + v(x,r,\theta) \\
q_\theta(x,r,\theta) &= U_\infty \sin\alpha \cos\theta + w(x,r,\theta)
\end{aligned}
\right\} \qquad (2)
$$

where U_∞ is the free-stream velocity and u, v, and w are the perturbation velocity components in the x-, r-, and θ-direction, respectively. The Cartesian perturbation velocity components in the y- and z-directions are designated as v_c and w_c, respectively.

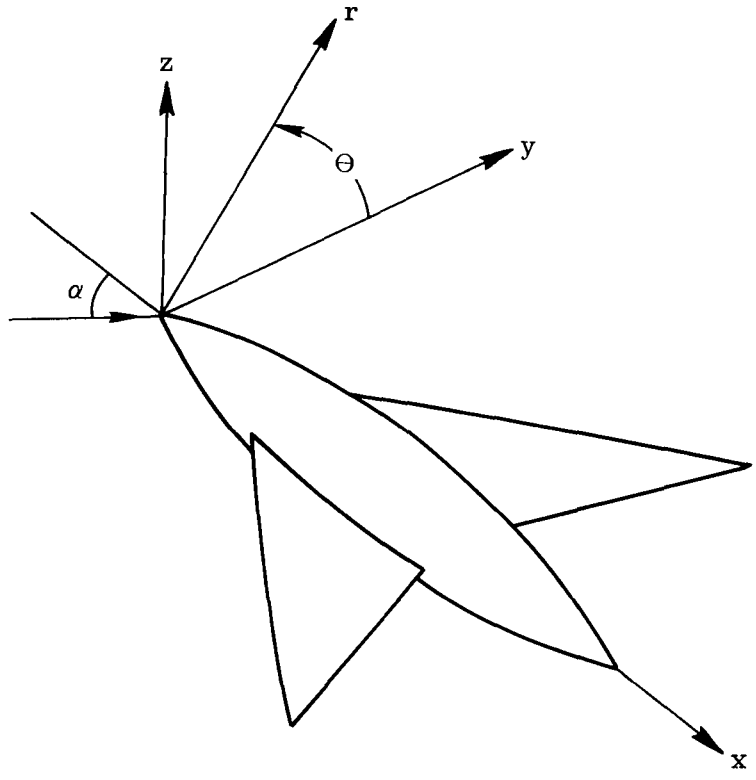

Figure 3.- Frame of reference.

Consider a wing-body combination composed of a slender axisymmetric body and a thin wing which passes through or near the body axis. It is assumed that the cross-sectional areas of the wing and body are, in general, of the same order of magnitude. Since the cross-sectional area of the wing is proportional to both t^2 and bt_w, the wing thickness can be expressed as

$$\left.\begin{aligned} t_w &= C_w \frac{t^2}{b} \\ C_w &= O(1) \end{aligned}\right\} \qquad (3)$$

The body radius r_b and wing thickness z_w, which are depicted in figure 4, are specified by the equations

$$r_b = t\, F(x) \qquad (4)$$

and

$$z_w = \ell \sin \alpha\, g(x,y) \pm t_w\, h(x,y) \qquad (5)$$

respectively, where the plus sign in equation (5) is used for the top surface of wing and the minus sign is used for the bottom surface. The function $F(x)$ is the nondimensional radius of the body, and the functions $g(x,y)$ and $h(x,y)$ give the twist and camber distribution and the thickness distribution of the wing, respectively. As shown in figure 4,

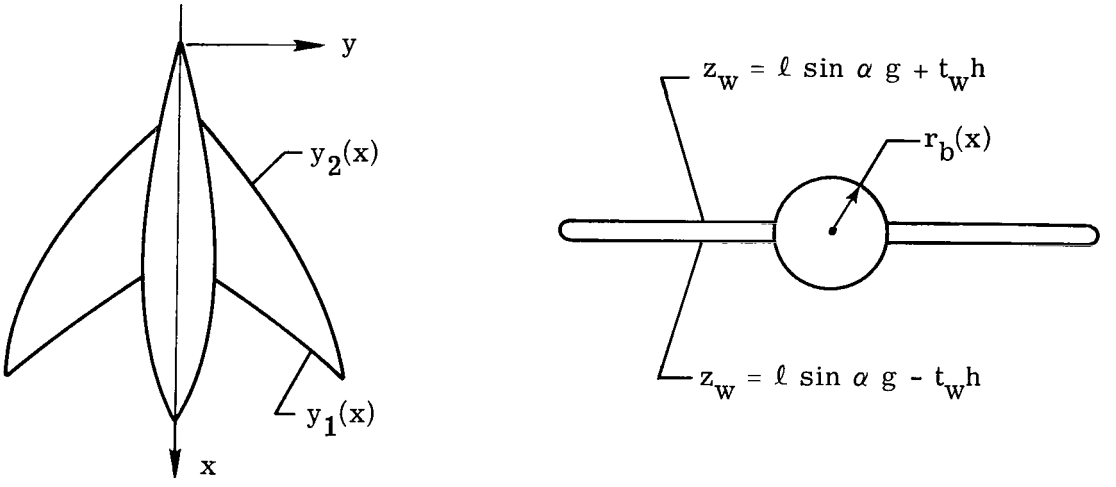

(a) Planform. (b) Cross section.

Figure 4.- Vehicle geometry.

the leading and trailing edges of the wing are specified by the functions $y_2(x)$ and $y_1(x)$, respectively. It is assumed that the wing twist and camber are scaled by the quantity $\ell \sin \alpha$ (that is, the order of magnitude of the twist and camber is assumed to be $\ell \sin \alpha$)

so that the effects of these quantities are of the same order of magnitude as those of angle of attack. The exact boundary conditions at the body and wing surfaces are

$$v\left(x,r_b,\theta\right) = -U_\infty \sin\alpha \sin\theta + \left[U_\infty \cos\alpha + u(x,r,\theta)\right] t \frac{dF(x)}{dx} \tag{6a}$$

and

$$w_c\left(x,y,z_w\right) = -U_\infty \sin\alpha + \left[U_\infty \cos\alpha + u\left(x,y,z_w\right)\right]\left[\ell \sin\alpha \frac{\partial g(x,y)}{\partial x} \pm t_w \frac{\partial h(x,y)}{\partial x}\right]$$

$$+ v_c\left(x,y,z_w\right)\left[\ell \sin\alpha \frac{\partial g(x,y)}{\partial y} \pm t_w \frac{\partial h(x,y)}{\partial y}\right] \tag{6b}$$

respectively.

It is assumed that the flow fields under consideration are isentropic. Although this assumption is not strictly valid when shock waves are present, it can be shown (ref. 10) that the largest term which is affected by the nonisentropic condition is of the order $\left(1 - M_\infty^2\right)^3$, which is very small for transonic flow. Hayes (ref. 5) and Cole and Messiter (ref. 11; also ref. 4) show that to the degree of approximation employed in this report, the isentropic assumption is valid.

If the flow is isentropic, the perturbation velocity potential φ can be defined so that

$$u = \frac{\partial\varphi}{\partial x}$$

$$v = \frac{\partial\varphi}{\partial r}$$

$$w = \frac{1}{r}\frac{\partial\varphi}{\partial\theta}$$

From equation (5.5) of reference 4, it can be shown that the exact partial differential equation governing φ is

$$\left(1 - M_\infty^2\right)\frac{\partial^2\varphi}{\partial x^2} + \frac{\partial^2\varphi}{\partial r^2} + \frac{1}{r}\frac{\partial\varphi}{\partial r} + \frac{1}{r^2}\frac{\partial^2\varphi}{\partial\theta^2} = M_\infty^2\left(\sin 2\alpha\left(\frac{\partial^2\varphi}{\partial x\,\partial r}\sin\theta + \frac{1}{r}\frac{\partial^2\varphi}{\partial x\,\partial\theta}\cos\theta\right) + \sin^2\alpha\left[-\frac{\partial^2\varphi}{\partial x^2} + \left(\frac{\partial^2\varphi}{\partial r^2}\sin\theta + \frac{1}{r}\frac{\partial^2\varphi}{\partial r\,\partial\theta}\cos\theta\right)\sin\theta\right.\right.$$

$$\left.\left. + \frac{1}{r}\left(\frac{\partial^2\varphi}{\partial r\,\partial\theta}\sin\theta + \frac{1}{r}\frac{\partial^2\varphi}{\partial\theta^2}\cos\theta\right)\cos\theta + \frac{1}{r}\left(\frac{\partial\varphi}{\partial r}\cos\theta - \frac{1}{r}\frac{\partial\varphi}{\partial\theta}\sin\theta\right)\cos\theta\right] + \frac{\cos\alpha}{U_\infty}\left[(\gamma + 1)\frac{\partial\varphi}{\partial x}\frac{\partial^2\varphi}{\partial x^2}\right.\right.$$

(Equation continued on next page)

$$+ 2\frac{\partial\varphi}{\partial r}\frac{\partial^2\varphi}{\partial x\partial r} + \frac{2}{r^2}\frac{\partial\varphi}{\partial\theta}\frac{\partial^2\varphi}{\partial x\partial\theta} + (\gamma - 1)\frac{\partial\varphi}{\partial x}\left(\frac{\partial^2\varphi}{\partial r^2} + \frac{1}{r}\frac{\partial\varphi}{\partial r} + \frac{1}{r^2}\frac{\partial^2\varphi}{\partial\theta^2}\right)\Bigg] + \frac{\sin\alpha}{U_\infty}\Bigg[(\gamma - 1)\left(\frac{\partial\varphi}{\partial r}\sin\theta\right.$$

$$\left. + \frac{1}{r}\frac{\partial\varphi}{\partial\theta}\cos\theta\right)\left(\frac{\partial^2\varphi}{\partial x^2} + \frac{\partial^2\varphi}{\partial r^2} + \frac{1}{r}\frac{\partial\varphi}{\partial r} + \frac{1}{r^2}\frac{\partial^2\varphi}{\partial\theta^2}\right) + 2\frac{\partial\varphi}{\partial r}\frac{\partial^2\varphi}{\partial r^2}\sin\theta + \frac{2}{r^3}\frac{\partial\varphi}{\partial\theta}\frac{\partial^2\varphi}{\partial\theta^2}\cos\theta$$

$$+ \frac{1}{r}\frac{\partial\varphi}{\partial\theta}\left(\frac{\partial\varphi}{\partial r}\cos\theta - \frac{1}{r}\frac{\partial\varphi}{\partial\theta}\sin\theta\right)\Bigg] + \frac{1}{U_\infty^2}\Bigg\{\left(\frac{\partial\varphi}{\partial r}\right)^2\frac{\partial^2\varphi}{\partial r^2} + \frac{1}{r^4}\left(\frac{\partial\varphi}{\partial\theta}\right)^2\frac{\partial^2\varphi}{\partial\theta^2} + 2\frac{\partial\varphi}{\partial x}\frac{\partial\varphi}{\partial r}\frac{\partial^2\varphi}{\partial x\partial r}$$

$$+ \frac{2}{r^2}\frac{\partial\varphi}{\partial x}\frac{\partial\varphi}{\partial\theta}\frac{\partial^2\varphi}{\partial x\partial\theta} + \frac{2}{r^2}\frac{\partial\varphi}{\partial r}\frac{\partial\varphi}{\partial\theta}\frac{\partial^2\varphi}{\partial r\partial\theta} + \left(\frac{\partial\varphi}{\partial x}\right)^2\frac{\partial^2\varphi}{\partial x^2} + \frac{\gamma - 1}{2}\Bigg[\left(\frac{\partial\varphi}{\partial x}\right)^2 + \left(\frac{\partial\varphi}{\partial r}\right)^2$$

$$\left. + \frac{1}{r^2}\left(\frac{\partial\varphi}{\partial\theta}\right)^2\Bigg]\left(\frac{\partial^2\varphi}{\partial x^2} + \frac{\partial^2\varphi}{\partial r^2} + \frac{1}{r}\frac{\partial\varphi}{\partial r} + \frac{1}{r^2}\frac{\partial^2\varphi}{\partial\theta^2}\right)\Bigg\}\Bigg) \tag{7}$$

Application of Method of Matched Asymptotic Expansions

This method is applicable to problems for which the characteristic length scale of disturbances in a limited region of interest, called the inner region, differs from that in the surrounding, or outer, region when one or more control parameters are small. As a result of this difference in length scales, the magnitudes of various terms in the governing equations differ in the two regions so that the approximate forms of the governing equations in the two regions are different. The formal procedure is to determine asymptotic expansions in the inner and outer regions and to match these expansions term by term according to the matching principle of Kaplun and Lagerstrom (ref. 12) in the zone where the two regions overlap. This matching of terms serves to determine coefficients and gage functions in the expansions. If the inner and outer regions do not overlap, as in the case for the problem treated in this report, the formal procedure includes the determination of a third expansion in an intermediate region which overlaps the inner and outer regions. This intermediate expansion is then matched to both the inner and the outer expansions. A detailed discussion of the method of matched asymptotic expansions has been given by Van Dyke (ref. 13).

The problem of transonic flow past lifting configurations with span-length ratios of order one is well suited for treatment with this method since the magnitude of the length scale in planes normal to the axis is the same as that of the span near the vehicle but is much larger than that of the span at large distances from the vehicle if the reduced semispan-length ratio $\sqrt{|1 - M_\infty^2|}\, b/\ell$ is small. In this report the length scales for the axial and radial coordinates in the inner region are chosen to be the configuration length ℓ and the semispan b, respectively. Therefore, the independent variables in this region are $\tilde{x}$, $\tilde{r}$, and θ where

$$\left.\begin{aligned} \tilde{x} &= \frac{x}{\ell} \\ \tilde{r} &= \frac{r}{b} \end{aligned}\right\} \tag{8}$$

The length scales for the axial and radial coordinates in the outer region are ℓ and ℓ/ν, respectively, where

$$\nu \ll 1$$

Thus, the independent variables in the outer region $\bar{x}$, $\bar{r}$, and θ are

$$\left.\begin{aligned} \bar{x} &= \frac{x}{\ell} = \tilde{x} \\ \bar{r} &= \frac{\nu r}{\ell} = \lambda \nu \tilde{r} \end{aligned}\right\} \tag{9}$$

where $\lambda = \frac{b}{\ell}$.

It will be shown that as indicated previously, the regions of validity of the inner and outer expansions for the present problem do not overlap. Consequently, an intermediate expansion is obtained and matched with the inner and outer expansions in order to show that the formal matching procedure of Kaplun and Lagerstrom (ref. 12) can be applied to this problem. However, it is first shown that the inner and outer expansions can be constructed with a less formal and also less complicated procedure. This procedure consists of the determination of the gage function of the leading term of the outer expansion in terms of the stretching parameter ν, the determination of the inner expansion for large values of the inner radial variable $\tilde{r}$, the transformation of this expansion to outer variables, and the matching of the gage function of the leading term in the transformed expansion to the known expression for the gage function of the leading term in the outer expansion.

Scaling of Basic Parameters

The relationships between the parameter ν, the free-stream Mach number M_∞, and the magnitude of the velocity potential in the outer region can be established from physical considerations. Let the expansion for the velocity potential in the outer region be written as

$$\varphi(x,r,\theta) = U_\infty \ell \sum_{i=1}^{\infty} \epsilon_i \, \Phi_i(\bar{x},\bar{r},\theta) \tag{10}$$

where

$$\epsilon_1 << 1$$

$$\epsilon_{i+1} << \epsilon_i$$

From equations (7), (9), and (10), it can be shown that the first approximation to the governing equation in the outer region is

$$(1 - M_\infty^2)\Phi_1'' + \nu^2\bar{\nabla}_2^2\Phi_1 = (\gamma + 1)\epsilon_1\Phi_1'\Phi_1'' \tag{11}$$

where $\bar{\nabla}_2^2$, the Laplace operator in planes normal to the x-axis in terms of outer variables, is written as

$$\bar{\nabla}_2^2 = \frac{\partial^2}{\partial\bar{r}^2} + \frac{1}{\bar{r}}\frac{\partial}{\partial\bar{r}} + \frac{1}{\bar{r}^2}\frac{\partial^2}{\partial\theta^2} \tag{12}$$

and where the prime denotes differentiation with respect to $\bar{x}$. If equation (11) is to be valid for completely subsonic and completely supersonic flows, the magnitudes of the terms on the left-hand side must be the same. If the sign of the coefficient of the derivative Φ_1'' in equation (11) is to change, as it must for transonic flow, the magnitude of the term on the right-hand side must be the same as that of the first term on the left. Consequently, the quantities $1 - M_\infty^2$, ν^2, and ϵ_1 in equation (11) must be of the same order of magnitude. In this report this fact is expressed as

$$\nu^2 = \epsilon_1 = \frac{1 - M_\infty^2}{K} \tag{13}$$

where K is an order-one constant. Note that equation (11) is, in general, of the mixed elliptic-hyperbolic type.

As noted in "Introduction," the outer regions of transonic flow fields about slender bodies at angles of attack of the order of the equivalent thickness ratio and about wing bodies with span-length ratios of order one at angles of attack of the order of the wing thickness are dominated by thickness effects. Oswatitsch and Keune (ref. 1) show that if thickness effects are dominant, the radial stretching parameter ν and the equivalent thickness ratio δ are of the same order of magnitude. It should be noted that it is common practice to equate these two quantities. In reference 9 Cheng and Hafez point out that it is physically realistic to assume that the relationship between ν and δ which is valid for thickness-dominated flows should also hold for flows where the effects of lift and thickness are comparable. Consequently, it is assumed in this report that ν and δ are related by the equation

$$\nu = \delta \tag{14}$$

if the effects of lift and thickness are of the same order of magnitude in the outer region and by the inequality

$$\nu >> \delta \tag{15}$$

if the effects of lift are dominant.

It should be noted that it remains to establish the relationship between the angle of attack α and the other basic parameters.

Inner Expansion

The perturbation velocity potential in the inner region may be written as

$$\varphi(x,r,\theta) = U_\infty \ell \left\{ \delta^2 \log_e\left(\frac{1}{\lambda\nu}\right) \varphi_{\delta,1}(\tilde{x},\tilde{r},\theta) + \delta^2 \varphi_\delta(\tilde{x},\tilde{r},\theta) + \lambda \sin\alpha\, \phi_1(\tilde{x},\tilde{r},\theta) \right.$$

$$\left. + \sum_{m=2}^{\infty} \lambda^{3m-2} \sin^m \alpha \left[\phi_m(\tilde{x},\tilde{r},\theta) + \sum_{n=1}^{m} \log_e^n\left(\frac{1}{\lambda\nu}\right) \phi_{m,n}(\tilde{x},\tilde{r},\theta) \right] \right\} \tag{16}$$

The first two terms are the usual lowest order thickness terms, the third term is the usual lowest order lift term, and the remaining terms are the higher order lift, thickness, and lift-thickness interaction terms. The thickness potentials have the leading subscript δ, and the potentials with gage functions proportional to $\sin^m \alpha$ have the leading subscript m. The potentials with gage functions proportional to $\log_e^n\left(\frac{1}{\lambda\nu}\right)$ have a second subscript n. Since a unique relationship can and will be established between the angle of attack α and the equivalent thickness ratio δ, it is possible to express all the gage functions in equation (16) in terms of only one of these parameters. In this report, however, the lowest order gage functions are expressed in terms of their respective natural parameters for purposes of simplicity. It will be shown that the gage functions of the thickness terms are of the same order of magnitude as those of some of the second-order lift terms.

The boundary conditions (eqs. (6)) can be expressed in terms of the component potentials of the inner expansion (eq. (16)) to second order in δ and $\sin\alpha$ as

$$\left.\begin{aligned} \frac{\partial \varphi_\delta(\tilde{x},\tilde{r}_b,\theta)}{\partial \tilde{r}} &= \frac{\lambda}{\delta}\frac{dF(\tilde{x})}{d\tilde{x}} \\ \frac{\partial \varphi_\delta(\tilde{x},\tilde{r},\pm 0)}{\partial \theta} &= -\frac{\partial \varphi_\delta(\tilde{x},\tilde{r},\pm\pi)}{\partial \theta} = \pm C_w \tilde{r}\frac{\partial h(\tilde{x},\tilde{y})}{\partial \tilde{x}} \end{aligned}\right\} \tag{17}$$

$$\left.\begin{aligned} \frac{\partial \phi_1(\tilde{x},\tilde{r}_b,\theta)}{\partial \tilde{r}} &= -\sin\theta \\ \frac{\partial \phi_1(\tilde{x},\tilde{r},0)}{\partial \theta} &= -\frac{\partial \phi_1(\tilde{x},\tilde{r},\pi)}{\partial \theta} = -\tilde{r}\left[1 - \frac{\partial g(\tilde{x},\tilde{y})}{\partial \tilde{x}}\right] \end{aligned}\right\} \tag{18}$$

$$\left.\begin{aligned} \frac{\partial \phi_2(\tilde{x},\tilde{r}_b,\theta)}{\partial \tilde{r}} &= 0 \\ \frac{\partial \phi_2(\tilde{x},\tilde{r},\pm 0)}{\partial \theta} &= -\frac{\partial \phi_2(\tilde{x},\tilde{r},\pm\pi)}{\partial \theta} = -\frac{\tilde{r}}{\lambda^2}\left[\frac{\partial \phi_1(\tilde{x},\tilde{r},\pm 0)}{\partial \tilde{x}}\frac{\partial g(\tilde{x},\tilde{y})}{\partial x} + \frac{1}{\lambda^2}\frac{\partial \phi_1(\tilde{x},\tilde{y},\pm 0)}{\partial \tilde{y}}\frac{\partial g(\tilde{x},\tilde{y})}{\partial \tilde{y}}\right] \end{aligned}\right\} \tag{19}$$

The potentials $\varphi_{\delta,1}$, $\phi_{2,1}$, and $\phi_{2,2}$ satisfy homogeneous Neumann boundary conditions.

The governing equations for the component potentials in the inner expansion (eq. (16)) are obtained after substitution of that expansion into equation (7) and collection of terms of the same magnitudes. It is found that the first-order potential ϕ_1 and all the second-order potentials except ϕ_2 satisfy the two-dimensional Laplace equation in the cross-flow plane. For example,

$$\tilde{\nabla}_2^2 \phi_1 = 0 \tag{20}$$

where

$$\tilde{\nabla}_2^2 = \frac{\partial^2}{\partial \tilde{r}^2} + \frac{1}{\tilde{r}}\frac{\partial}{\partial \tilde{r}} + \frac{1}{\tilde{r}^2}\frac{\partial^2}{\partial \theta^2} \tag{21}$$

The potential ϕ_2 satisfies the Poisson equation

$$\tilde{\nabla}_2^2 \phi_2 = (\gamma + 1)\phi_1'\phi_1'' + \frac{2}{\lambda^2}\left(\frac{\partial \phi_1'}{\partial \tilde{r}}\sin\theta + \frac{1}{\tilde{r}}\frac{\partial \phi_1'}{\partial \theta}\cos\theta + \frac{\partial \phi_1}{\partial \tilde{r}}\frac{\partial \phi_1'}{\partial \tilde{r}} + \frac{1}{\tilde{r}^2}\frac{\partial \phi_1}{\partial \theta}\frac{\partial \phi_1'}{\partial \theta}\right) \tag{22}$$

The governing equations for the higher order potentials are discussed subsequently. It is interesting to note that the governing equations of the inner potentials are all parabolic since the determinant of the second-order coefficient matrix vanishes for each of these equations. (See ref. 14.)

First-order potential.- The governing equation and boundary conditions for the first-order potential ϕ_1 are given by equations (20) and (18), respectively. Solutions for this potential, which are traditionally termed slender-wing solutions, have been obtained previously for the three wing-body configurations depicted in figure 5.

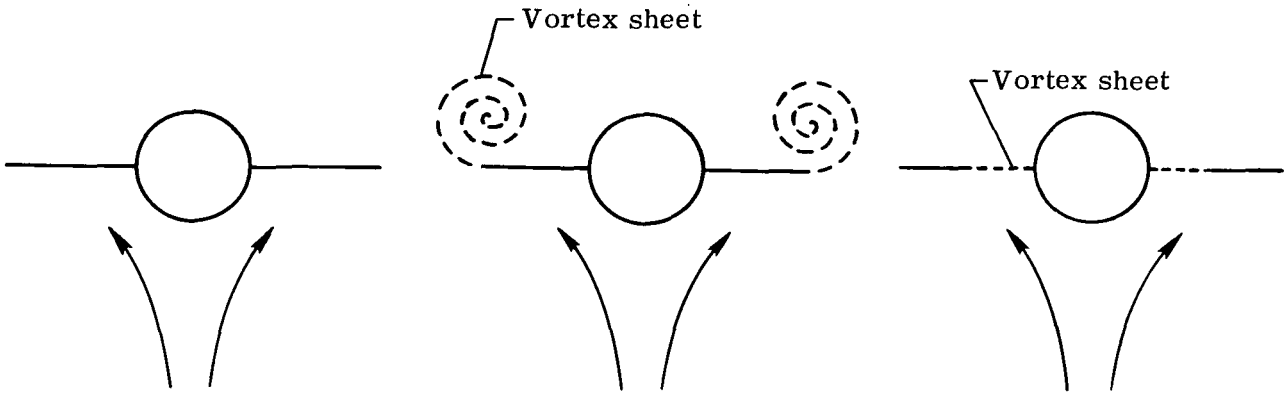

(a) Attached leading-edge flow.

(b) Separated leading-edge flow.

(c) Attached leading-edge flow; swept trailing edge.

Figure 5.- Wing-body configurations with known slender-wing cross-flow solutions.

In this report flows in which the lower surface-wetting streamlines which approach the leading edge separate from the surface at the leading edge are termed separated leading-edge flows. Flows in which the surface-wetting streamlines remain attached to the surface are termed attached leading-edge flows. The solution for attached leading-edge flow past wing-body configurations with flat wings with straight trailing edges (fig. 5(a)) was obtained by Spreiter (ref. 15) and Ward (ref. 16). It should be noted that this solution is an extension of the basic slender-wing solution obtained by Jones (ref. 17). The solution for separated leading-edge flow past configurations of the same type (fig. 5(b)) was obtained by Wei, Levinsky, and Su (ref. 18) and is an extension of the work done by Mangler and Smith (ref. 19) and Smith (ref. 20) on separated leading-edge flow past slender flat-plate delta wings. The solution for attached leading-edge flow past wing-body configurations with flat-plate wings with swept leading and trailing edges (fig. 5(c) was developed by Mirels (ref. 21) and Mangler (ref. 22). These solutions are reviewed in appendix A.

No slender-wing solution for separated leading-edge flow past a wing with a swept trailing edge is known to the author.

As mentioned previously, the inner and outer expansions are to be matched in the region where the inner radial variable $\tilde{r}$ is large. In appendix A it is shown that in the region beyond the wing where $\tilde{r} >> \tilde{y}_2(\tilde{x})$, the potential ϕ_1 can be written as

$$\phi_1(\tilde{x},\tilde{r},\theta) = f(\tilde{x}) \frac{\sin \theta}{\tilde{r}} \tag{23}$$

For the configurations in figures 5(a) and 5(b), which have swept leading edges only,

$$f(\tilde{x}) = \frac{1}{2} \tilde{y}_2^2(\tilde{x}) \tag{24}$$

where $y_2(x)$ is the function for the leading edge of the wing. It is shown in appendix A that this equation is valid to lowest order for both attached and separated leading-edge flow. For the configuration in figure 5(c), which has both swept leading and swept trailing edges, the function f satisfies the equation

$$f'(\tilde{x}) = S(\tilde{x}) \left[1 - \frac{E(k)}{K(k)}\right] \tilde{y}_2(\tilde{x}) \, \tilde{y}_2'(\tilde{x}) \tag{25}$$

where K and E are complete elliptic integrals of the first and second kinds, respectively, with the argument

$$k(\tilde{x}) = \sqrt{1 - \frac{\tilde{y}_1^2(\tilde{x})}{\tilde{y}_2^2(\tilde{x})}} \tag{26}$$

The quantity $S(\tilde{x})$ is the same as the function S used by Mirels (see section 4 of ref. 21) and H used by Mangler (see section 3 of ref. 22) for wings with swept trailing edges. It is shown in appendix B that for configurations with twisted and cambered wings, the function f can be approximated as

$$f(\tilde{x}) = \frac{1}{2} \tilde{y}_2^2(\tilde{x}) - \frac{2}{\pi} \int_{\eta=\tilde{r}_b(\tilde{x})}^{\eta=\tilde{y}_2(\tilde{x})} g'(\tilde{x},z) \sqrt{\tilde{y}_2^2(\tilde{x}) - \eta^2} \, d\eta \tag{27}$$

if only the leading edge of the wing is swept. It is also shown that if both the leading and trailing edges of the wing are swept, the derivative $f'(\tilde{x})$ is approximately

$$f'(\tilde{x}) = S(\tilde{x}) \left[1 - \frac{E(k)}{K(k)}\right] \tilde{y}_2(\tilde{x}) \, \tilde{y}_2'(\tilde{x}) - \frac{1}{\pi} B_o(\tilde{x}) \tag{28}$$

where the modulus of K and E is given by equation (26). The function $B_0(\tilde{x})$ is the same as the function B used by Klunker and Harder (ref. 23). The determination of this function is discussed in section 2 of reference 23.

In the region very near the wing, the potential ϕ_1 can be expressed in the form

$$\phi_1(\tilde{x},\tilde{y},z) = m_{\pm}(\tilde{x},\tilde{y}) - \left[1 - \frac{\partial g(\tilde{x},\tilde{y})}{\partial \tilde{x}}\right]\tilde{z} \tag{29}$$

in order to satisfy boundary conditions (eqs. (18)). This form of the potential is used in the determination of the surface flow properties and some of the higher order terms. The upper and lower signs in equation (29) apply on the leeward and windward sides of the wing, respectively.

Thickness potentials.- The terms in the inner expansion (eq. (16)) involving the thickness potentials φ_δ and $\varphi_{\delta,1}$ are of second order in that the gage functions of these terms are δ^2 and $\delta^2 \log_e(1/\lambda\nu)$, respectively. Both potentials are governed by the two-dimensional Laplace equation in the cross-flow plane. The potential φ_δ satisfies boundary conditions (eqs. (17)) and the potential $\varphi_{\delta,1}$ satisfies homogeneous Neumann boundary conditions.

It has been shown by Stocker (ref. 24) that the solution for φ_δ is

$$\varphi_\delta(\tilde{x},\tilde{r},\theta) = g_\delta(\tilde{x}) + \psi(\tilde{x},\tilde{r},\theta)$$

where

$$\psi(\tilde{x},\tilde{r},\theta) = F(\tilde{x})\,F'(\tilde{x}) - \frac{2C_w}{\pi\lambda}\int_{\eta=\tilde{r}_b(\tilde{x})}^{\eta=\tilde{y}_2(\tilde{x})} h'(\tilde{x},\eta)\,d\eta$$

$$+ \frac{C_w}{\pi\lambda}\int_{\eta=\tilde{r}_b(\tilde{x})}^{\eta=\tilde{y}_2(\tilde{x})} h'(\tilde{x},\eta)\left\{\log_e\sqrt{\left(\tilde{r}^2+\eta^2\right)^2 - 4\tilde{r}^2\eta^2\cos^2\theta}\right.$$

$$\left. + \log_e\sqrt{\left(\tilde{r}^2 + \frac{r_b^4(\tilde{x})}{\eta^2}\right)^2 - \frac{4\tilde{r}^2\tilde{r}_b^4(\tilde{x})}{\eta^2}\cos^2\theta}\right\} d\eta \tag{30}$$

For $\tilde{r} \gg \tilde{y}_2(\tilde{x})$, equation (30) can be approximated as

$$\psi = F_e(\tilde{x})\,F_e'(\tilde{x})\log_e\tilde{r}$$

where $F_e(\tilde{x})$, the nondimensional thickness distribution of the axisymmetric body with the same cross-sectional area, is written as

$$F_e(\tilde{x}) = \sqrt{F^2(\tilde{x}) + \frac{4C_w}{\pi\lambda} \int_{\eta=\tilde{r}_b(\tilde{x})}^{\eta=\tilde{y}_2(\tilde{x})} h'(\tilde{x},\eta)\, d\eta} \tag{31}$$

Since the governing equation and boundary conditions for $\varphi_{\delta,1}$ are homogeneous and are expressed in terms of the independent variables in the cross-flow plane, this potential can only depend on the independent variable $\tilde{x}$. Oswatitsch and Keune (ref. 1) have shown that if the leading term in the outer expansion depends on the thickness, as is the case for flows which are thickness dominated and flows for which the effects of lift and thickness are comparable, the potential $\varphi_{\delta,1}$ is determined when the inner and outer expansions are matched. With equations (9) the thickness part of the inner expansion (eq. (16)) can be written in terms of outer variables for large values of the inner radial variable $\tilde{r}$ as

$$\delta^2 \log_e\left(\frac{1}{\lambda\nu}\right)\varphi_{\delta,1}(\tilde{x}) + \delta^2\left[g_\delta(\tilde{x}) + F_e(\tilde{x})\, F_e'(\tilde{x}) \log_e \tilde{r}\right] = \delta^2 \log_e\left(\frac{1}{\lambda\nu}\right)\left[\varphi_{\delta,1}(\bar{x}) + F_e(\bar{x})\, F_e'(\bar{x})\right]$$

$$+ \delta^2\left[g_\delta(\bar{x}) + F_e(\bar{x})\, F_e'(\bar{x}) \log_e \bar{r}\right] \tag{32}$$

It has already been shown that if the leading term in the outer expansion depends on thickness, the gage function of this term can be written as

$$\epsilon_1 = \nu^2 = \delta^2$$

It follows that the leading term on the right-hand side of equation (32) must be zero so that

$$\varphi_{\delta,1} = -F_e F_e' \tag{33}$$

Second-order lift potentials.- The potentials $\phi_{2,1}$ and $\phi_{2,2}$ are governed by the two-dimensional Laplace equation in the cross-flow plane and satisfy homogeneous Neumann boundary conditions. Consequently, these potentials are functions of the independent variable $\tilde{x}$ only and can be written as

$$\left.\begin{aligned} \phi_{2,1} &= g_{2,1}(\tilde{x}) \\ \phi_{2,2} &= g_{2,2}(\tilde{x}) \end{aligned}\right\} \tag{34}$$

The potential ϕ_2 is governed by equation (22), a Poisson equation, and satisfies boundary conditions (eqs. 19)). The particular solution for ϕ_2 was first presented in reference 8. This solution, which was derived for large values of the inner radial variable in terms of wind-oriented coordinates, is written in terms of the body-oriented coordinates used in this report as

$$\phi_2^P = \frac{\gamma + 1}{4} f'(\tilde{x})\, f''(\tilde{x}) \log_e^2 \tilde{r} - \frac{1}{2} f'(\tilde{x}) \left[\frac{1}{\lambda^2} - \frac{\gamma + 1}{4} f''(\tilde{x}) \right] \cos 2\theta + \frac{f(\tilde{x})\, f'(\tilde{x})}{2\lambda^2 \tilde{r}^2} \tag{35}$$

In reference 9 Cheng and Hafez present the solution for ϕ_2 in terms of wind-oriented coordinates in a form which is not restricted to large values of the inner radial variable. This solution is derived in detail in reference 25. The solution in terms of body-oriented coordinates can be obtained in a similar manner. Let the potential ϕ_2 be written as

$$\phi_2 = g_2 + \phi_{2a} + \phi_{2b} + \phi_{2c} + \phi_{2d} \tag{36}$$

where the potentials ϕ_{2a}, ϕ_{2b}, and ϕ_{2c} are governed by the Poisson equations

$$\tilde{\nabla}_2^2 \phi_{2a} = (\gamma + 1)\phi_1' \phi_1'' \tag{37}$$

$$\tilde{\nabla}_2^2 \phi_{2b} = \frac{2}{\lambda^2} \left(\frac{\partial \phi_1}{\partial \tilde{r}} \frac{\partial \phi_1'}{\partial \tilde{r}} + \frac{1}{\tilde{r}^2} \frac{\partial \phi_1}{\partial \theta} \frac{\partial \phi_1'}{\partial \theta} \right) \tag{38}$$

$$\tilde{\nabla}_2^2 \phi_{2c} = \frac{2}{\lambda^2} \left(\frac{\partial \phi_1'}{\partial \tilde{r}} \sin \theta + \frac{1}{\tilde{r}} \frac{\partial \phi_1'}{\partial \theta} \cos \theta \right) \tag{39}$$

and satisfy homogeneous Neumann boundary conditions. The potential ϕ_{2d} is governed by the two-dimensional Laplace equation in the cross-flow plane and satisfies the boundary conditions

$$\left.\begin{aligned} &\frac{\partial \phi_{2d}(\tilde{x},\tilde{r}_b,\theta)}{\partial \tilde{r}} = 0 \\ &\frac{\partial \phi_{2d}(\tilde{x},\tilde{r},\pm 0)}{\partial \theta} = -\frac{\partial \phi_{2d}(\tilde{x},\tilde{r},\pm \pi)}{\partial \theta} = \mp \frac{\tilde{r}}{\lambda^2} \left[\frac{\partial \phi_1(\tilde{x},\tilde{y},+0)}{\partial \tilde{x}} \frac{\partial g(\tilde{x},\tilde{y})}{\partial \tilde{x}} + \frac{1}{\lambda^2} \frac{\partial \phi_1(\tilde{x},\tilde{y},+0)}{\partial \tilde{y}} \frac{\partial g(\tilde{x},\tilde{y})}{\partial \tilde{y}} \right] \end{aligned}\right\} \tag{40}$$

Consider the particular solution of ϕ_{2a} and ϕ_{2b}. Let the complex variables in the cross-flow plane in terms of inner variables be

$$X = \tilde{r}e^{i\theta}$$

and let the complex conjugate of X be designated as X^*. Equations (37) and (38) can be written as

$$\frac{\partial^2 \phi_{2a}}{\partial X \partial X^*} = \frac{\partial}{\partial \tilde{x}} \left(\phi_1'\right)^2 \tag{41}$$

and

$$\frac{\partial^2 \phi_{2b}}{\partial X \partial X^*} = \frac{1}{\lambda^2} \frac{\partial \phi_1}{\partial X} \frac{\partial \phi_1}{\partial X^*} \tag{42}$$

respectively. Cheng and Hafez (refs. 9 and 25) show that the general form of the particular solutions to equations (41) and (42) are

$$\phi_{2a}^P = \frac{\gamma + 1}{8} \frac{\partial}{\partial \tilde{x}} \int dX \int dX^* \left[\phi_1'(x,X,X^*)\right]^2 \tag{43}$$

$$\phi_{2b}^P = \frac{1}{\lambda^2} \phi_1 \phi_1' \tag{44}$$

More detailed forms of these solutions are given in references 9 and 25 and in appendix C of this report.

It should be noted that the potential ϕ_{2c} appears in the present treatment and not in that of references 9 and 25 because body-oriented coordinates are used in the former case and wind-oriented coordinates in the latter. Equation (39) can be written in terms of Cartesian coordinates as

$$\frac{\partial^2 \phi_{2c}}{\partial \tilde{y}^2} + \frac{\partial^2 \phi_{2c}}{\partial \tilde{z}^2} = \frac{2}{\lambda^2} \frac{\partial \phi_1}{\partial \tilde{z}} \tag{45}$$

The particular solution to equation (45) is

$$\phi_{2c}^P = \frac{1}{\lambda^2} \tilde{z} \phi_1 \tag{46}$$

It has been shown by Cheng and Hafez (ref. 9) that the particular solutions ϕ_{2a}^P and ϕ_{2b}^P do not satisfy the appropriate boundary conditions. It is shown in appendix C that the particular solution ϕ_{2c} does not satisfy the boundary conditions either. In order to enforce the boundary conditions, it is necessary to include the complementary solutions. In reference 25 Cheng and Hafez derive the complementary solutions ϕ_{2a}^C

and ϕ_{2b}^{C} subject to the assumption that the presence of the body can be ignored. This assumption can be made since the body radius is, in general, small compared with the wing span so that the terms depending on the body radius are of higher order. The general form of the potential ϕ_{2a}^{C} is written as

$$\phi_{2c}^{C} = -\frac{1}{8\pi}\int_{s=-\tilde{y}_2}^{s=\tilde{y}_2}\left[\frac{\partial\phi_{2a}^{P}(\tilde{x},s,+0)}{\partial\tilde{z}} - \frac{\partial\phi_{2a}^{P}(\tilde{x},s,-0)}{\partial\tilde{z}}\right]\log_e\left[(s - X)(s - X^*)\right]ds \tag{47}$$

Similar expressions pertain for the potentials ϕ_{2b}^{C} and ϕ_{2c}^{C}. Detailed expressions for these solutions are given in appendix C. It should be noted that it is shown in reference 25 that in order for the solution ϕ_{2a}^{C} to exist, the derivative ϕ_1' must be differentiable in y at all points on the wing. This condition is not met, in general, by attached-flow solutions for ϕ_1. The solution for ϕ_{2a} derived in references 9 and 25 was restricted to attached flow past wings with leading edges which are drooped in such a manner that the differentiability condition is met. Consequently, there is at most one angle of attack for a given wing at which a solution can be obtained. In appendix C it is shown that the solution presented in references 9 and 25 is also valid for separated leading-edge flow at arbitrary angles of attack.

The potential ϕ_{2d}, which is governed by the two-dimensional Laplace equation and satisfies boundary conditions (eqs. (40)), is written as

$$\phi_{2d} = -\frac{1}{4\pi\lambda^2}\int_{s=-\tilde{y}_2(\tilde{x})}^{s=\tilde{y}_2(\tilde{x})}\left[m'(\tilde{x},s)\,g'(\tilde{x},s) + \frac{1}{\lambda^2}\frac{\partial m(\tilde{x},s)}{\partial\tilde{y}}\frac{\partial g(\tilde{x},s)}{\partial\tilde{y}}\right]\log_e\left[(s - X)(s - X^*)\right]ds \tag{48}$$

where

$$m(\tilde{x},\tilde{y}) = \frac{1}{2}\left[m_+(\tilde{x},\tilde{y}) - m_-(\tilde{x},\tilde{y})\right] \tag{49}$$

The presence of the body has been ignored as before. It should be noted that the potential ϕ_{2d} does not appear explicitly in the treatments of references 9 and 25 because the lift potential is not resolved into first- and second-order parts in those references.

From the results of appendix C, it is seen that for $\tilde{r} >> \tilde{y}_2(\tilde{x})$, the potential ϕ_2 is the sum of the potentials ϕ_2^{P} and ϕ_2^{C} where ϕ_2^{P} is given by equation (35) and ϕ_2^{C} is written as

$$\phi_2^C = g_2(\tilde{x}) - \frac{f(\tilde{x})\, f'(\tilde{x})}{4\lambda^2} \frac{\cos 2\theta}{\tilde{r}^2} + H(\tilde{x}) \log_e \tilde{r} \tag{50}$$

where the coefficient $H(\tilde{x})$ is

$$H(\tilde{x}) = \frac{\gamma + 1}{16\pi} \frac{\partial}{\partial \tilde{x}} \int_{s=-\tilde{y}_2(\tilde{x})}^{s=\tilde{y}_2(\tilde{x})} \gamma'(\tilde{x},s)\ \text{P.V.} \int_{t=-\tilde{y}_2(\tilde{x})}^{t=\tilde{y}_2(\tilde{x})} \gamma'(\tilde{x},t) \left(\frac{s}{t-s} + \log_e |t-s| \right) dt\, ds$$

$$- \frac{1}{2\pi\lambda^2} \int_{s=-\tilde{y}_2(\tilde{x})}^{s=\tilde{y}_2(\tilde{x})} m(\tilde{x},s)\, ds - \frac{1}{2\pi\lambda^2} \int_{s=-\tilde{y}_2(\tilde{x})}^{s=\tilde{y}_2(\tilde{x})} \left[m'(\tilde{x},s)\, g'(\tilde{x},s) + \frac{1}{\lambda^2} \frac{\partial m(\tilde{x},s)}{\partial \tilde{y}} \frac{\partial g(\tilde{x},s)}{\partial \tilde{y}} \right] ds$$

$$- \frac{1}{2\pi\lambda^2} \int_{s=-\tilde{y}_2(\tilde{x})}^{s=\tilde{y}_2(\tilde{x})} \left\{ m(\tilde{x},s)\, g''(\tilde{x},s) - m'(\tilde{x},s) \left[1 - g'(\tilde{x},s) \right] \right\} ds \tag{51}$$

The function $\gamma(\tilde{x},\tilde{y})$ is the wing vorticity at the point $\tilde{x},\tilde{y}$.

The relationship between the radial stretching parameter ν and the angle of attack α for flows for which the effects of lift are either dominant or comparable with the effects of thickness can be determined from a study of the second-order lift potentials. It can be shown from equations (9), (34), (35), and (50) that the sum of the second-order lift terms in the inner expansion can be written in terms of outer variables for large values of the inner radial variable $\tilde{r}$ as

$$\lambda^4 \sin^2\alpha \left[\log_e^2\left(\frac{1}{\lambda\nu}\right) \phi_{2,2}(\bar{x}) + \log_e\left(\frac{1}{\lambda\nu}\right) \phi_{2,1}(\bar{x}) + \phi_2(\bar{x},\bar{r},\theta) \right] = \lambda^4 \sin^2\alpha \log_e^2\left(\frac{1}{\lambda\nu}\right) \left[g_{2,2}(\bar{x}) + \frac{\gamma+1}{4} f'(\bar{x})\, f''(\bar{x}) \right] + \lambda^4 \sin^2\alpha \log_e\left(\frac{1}{\lambda\nu}\right)$$

$$\times \left[g_{2,1}(\bar{x}) + H(\bar{x}) + \frac{\gamma+1}{2} f'(\bar{x})\, f''(\bar{x}) \log_e \bar{r} \right] + \lambda^4 \sin^2\alpha \left\{ g_2(\bar{x}) + H(\bar{x}) \log_e \bar{r} \right.$$

$$\left. + \frac{\gamma+1}{4} f'(\bar{x})\, f''(\bar{x}) \log_e^2 \bar{r} - \frac{1}{2} f'(\bar{x}) \left[\frac{1}{\lambda^2} - \frac{\gamma+1}{4} f''(\bar{x}) \right] \cos 2\theta \right\} + \ldots \tag{52}$$

If the effects of lift are to influence the first term in the outer expansion, the gage function of the leading nonvanishing term on the right-hand side of equation (52) must be equal to ϵ_1. It has been shown that the parameter ν can be related to ϵ_1 by equation (13). In reference 8 it was assumed that none of the terms on the right-hand side of equation (52) vanish. This assumption led to the conclusion that α was related to λ and ν by the equation

$$\sin \alpha = \frac{a\nu}{\lambda^4 \log_e \frac{1}{\lambda\nu}}$$

where a is an order-one constant. In addition, it necessarily followed that if the effects of lift and thickness were comparable, δ was related to λ and ν by the equation

$$\delta^2 = \frac{\mu\nu^2}{\log_e \frac{1}{\lambda\nu}}$$

where μ is an order-one constant, rather than by equation (14). In reference 9 Cheng and Hafez present a second solution in which it is assumed that the first term in equation (52) vanishes identically. Consequently, the function $g_{2,2}(x)$ satisfies the equation

$$g_{2,2} = -\frac{\gamma + 1}{4} f'f'' \tag{53}$$

and α can be related to λ and ν by the equation

$$\sin \alpha = \frac{a\nu}{\lambda^2 \sqrt{\log_e \frac{1}{\lambda\nu}}} \tag{54}$$

It also follows that ν and δ can be related by equation (14) for the case where the effects of lift and thickness are comparable in the outer region. It is felt that this second solution is physically more realistic and, as a result, is the one used in this report.

Higher order potentials.- In the strictest sense, the acceptance of equations (53) and (54) should be contingent on the proof that these equations, when transformed to outer variables with equations (9), do not cause the higher order terms in the inner expansion for large values of the inner radial variable to appear to be of lower order than ϵ_1. It is shown in appendix D that the sum of the transformed third-order terms in the inner expansion is not, in fact, of lower order than ϵ_1. The same relationship can be shown to hold for the sums of the fourth and higher order terms of the inner expansion. Consequently, it can be concluded that equations (53) and (54) are acceptable and that the inner expansion for large values of $\tilde{r}$ can be written as

$$\Phi = \lambda \sin\alpha\, f(\tilde{x}) \frac{\sin\theta}{\tilde{r}} - \delta^2 \log_e\left(\frac{1}{\lambda\nu}\right) F_e(\tilde{x})\, F_e'(\tilde{x}) + \delta^2 \left[g_\delta(\tilde{x}) + F_e(\tilde{x})\, F_e'(\tilde{x}) \log_e \tilde{r} \right] - \lambda^4 \sin^2\alpha \log_e^2\left(\frac{1}{\lambda\nu}\right) \frac{\gamma + 1}{4} f'(\tilde{x})\, f''(\tilde{x})$$

$$+ \lambda^4 \sin^2\alpha \log_e\left(\frac{1}{\lambda\nu}\right) g_{2,1}(\tilde{x}) + \lambda^4 \sin^2\alpha \left\{ g_2(\tilde{x}) + H(\tilde{x}) \log_e \tilde{r} + \frac{f(\tilde{x})\, f'(\tilde{x})}{4\lambda^2} \frac{1 - \cos 2\theta}{\tilde{r}^2} + \frac{\gamma + 1}{4} f'(\tilde{x})\, f''(\tilde{x}) \log_e^2 \tilde{r} \right.$$

$$\left. - \frac{1}{2} f'(\tilde{x}) \left[\frac{1}{\lambda^2} - \frac{\gamma + 1}{4} f''(\tilde{x}) \right] \cos 2\theta \right\} + \ldots \tag{55}$$

Outer Expansion

Equation (10) gives the form of the outer expansion. It has already been shown that the gage function of the leading term is related to the radial stretching parameter ν (the reciprocal of the nondimensional radial length scale in the outer region) by equation (13). The higher order gage functions in the outer expansion can be determined from an observation of the inner expansion written in terms of outer variables for large values of the inner radial variable $\tilde{r}$. From equation (55), it is seen that this expression is written as

$$\Phi = \nu^2\left\{g_\delta(\bar{x}) + g_{2,1}(\bar{x}) + a^2 H(\bar{x}) + \left[F_e(\bar{x})\, F_e'(\bar{x}) + \frac{\gamma+1}{2} a^2 f'(\bar{x})\, f''(\bar{x})\right]\log_e \bar{r}\right\}$$

$$+ \frac{\nu^2 a}{\sqrt{\log_e \frac{1}{\lambda\nu}}}\frac{f(\bar{x})\sin\theta}{\bar{r}} + \frac{\nu^2 a^2}{\log_e \frac{1}{\lambda\nu}}\left\{g_2(\bar{x}) + H(\bar{x})\log_e \bar{r} + \frac{\gamma+1}{4} f'(\bar{x})\, f''(\bar{x})\log_e^2 \bar{r}\right.$$

$$\left. + \frac{1}{2} f'(\bar{x})\left[\frac{1}{\lambda^2} - \frac{\gamma+1}{4} f''(\bar{x})\right]\cos 2\theta\right\} + \ldots \tag{56}$$

It is seen from equation (56) that ϵ_2 and ϵ_3 are given by the equations

$$\epsilon_2 = \frac{\nu^2 a}{\sqrt{\log_e \frac{1}{\lambda\nu}}} \tag{57}$$

$$\epsilon_3 = \frac{\nu^2 a^2}{\log_e \frac{1}{\lambda\nu}} \tag{58}$$

The governing equation for the potential Φ_1 determined by the substitution of equation (13) into equation (11) is

$$K\Phi_1'' + \bar{\nabla}_2^2\Phi_1 = (\gamma+1)\Phi_1'\Phi_1'' \tag{59}$$

When expansion (eq. (10)) is substituted into equation (7) and the gage functions ϵ_1, ϵ_2, and ϵ_3 are specified by equations (13), (57), and (58), it is found that the potentials Φ_2 and Φ_3 are governed by the equations

$$K\Phi_2'' + \bar{\nabla}_2^2\Phi_2 = (\gamma+1)\left(\Phi_1'\Phi_2'\right)' + \frac{2}{\lambda^2}\left(\frac{\partial\Phi_1'}{\partial\bar{r}}\sin\theta + \frac{1}{\bar{r}}\frac{\partial\Phi_1'}{\partial\theta}\cos\theta\right) \tag{60}$$

$$K\Phi_3'' + \bar{\nabla}_2^2\Phi_3 = (\gamma + 1)\left[\left(\Phi_1'\Phi_3'\right)' + \Phi_2'\Phi_2''\right] + \frac{2}{\lambda^2}\left(\frac{\partial\Phi_2'}{\partial\bar{r}}\sin\theta + \frac{1}{\bar{r}}\frac{\partial\Phi_2'}{\partial\theta}\cos\theta\right) - \frac{1}{\lambda^2}\Phi_1'' \tag{61}$$

As pointed out by Messiter (ref. 4), equations of this type can be solved iteratively for $\bar{r} << 1$. For example, equation (59) is written in the form

$$\bar{\nabla}_2^2\Phi_1 = -K\Phi_1'' + (\gamma + 1)\Phi_1'\Phi_1'' \tag{62}$$

First, the pertinent complementary solution for $\bar{r} << 1$ is obtained as

$$\Phi_1 = G_1(\bar{x}) + A(\bar{x})\log_e\bar{r} \tag{63}$$

where the functions $G_1(\bar{x})$ and $A(\bar{x})$ are not yet known. A higher order solution is obtained after substitution of equation (63) in the right-hand side of equation (62) and integration of the resulting Poisson equation. The solution can then be written as

$$\Phi_1 = G_1(\bar{x}) + A(\bar{x})\log_e\bar{r} + \frac{\gamma + 1}{4}A'A''\bar{r}^2\log_e^2\bar{r} - \left\{\frac{K}{4}A'' + \frac{\gamma + 1}{2}\left[A'A'' - \frac{1}{2}\left(G_1'A'\right)'\right]\right\}\bar{r}^2\log_e\bar{r} - \left\{\frac{K}{4}G_1'' - \frac{\gamma + 1}{4}\left[\frac{3}{2}A'A'' - \left(G_1'A'\right)' + G_1'G_1''\right]\right\}\bar{r}^2 + \ldots \tag{64}$$

This procedure can be continued to higher orders if necessary. The pertinent solutions to equations (60) and (61) are found, in similar fashion, to be

$$\Phi_2 = B(\bar{x})\frac{\sin\theta}{\bar{r}} + \left\{A' - \frac{K}{2}B'' + \frac{\gamma + 1}{2}\left[B'\left(G_1' - \frac{1}{2}A'\right)\right]'\right\}\bar{r}\log_e\bar{r}\sin\theta + \frac{\gamma + 1}{4}\left(B'A'\right)'\bar{r}\log_e^2\bar{r}\sin\theta + \ldots \tag{65}$$

$$\Phi_3 = G_3(\bar{x}) + C_1(\bar{x})\log_e\bar{r} + \frac{\gamma + 1}{4}B'B''\log_e^2\bar{r} - \frac{B'}{2}\left(\frac{1}{\lambda^2} - \frac{\gamma + 1}{4}B''\right)\cos 2\theta + \ldots \tag{66}$$

where the functions $G_3(\bar{x})$, $B(\bar{x})$, and $C(\bar{x})$ are, at this point, arbitrary.

Matching of Expansions

Most of the unknown functions of x in the inner and outer expansions can be determined from a matching of the inner expansions for large values of the inner radial variable

$(\tilde{r} >> \tilde{y}_2)$ with the outer expansion for small values of the outer radial variable ($\bar{r} << 1$). As pointed out previously, there are two ways to accomplish the matching, by inspection and by the term-by-term procedure which has been formalized by Kaplun and Lagerstrom (ref. 12).

In this section these two expansions will be matched initially by inspection because of the simplicity of this method. It will then be evident that the regions of validity of the two expansions do not overlap. In order to satisfy the traditional requirement (which is sufficient but not necessary) that the matching of two expansions be done in a region of common validity, an intermediate expansion with a region of validity which overlaps those of the inner and outer expansions will be introduced. This intermediate expansion will be matched individually with the inner and outer expansions. It will then be seen that the expressions obtained for the inner and outer expansions with the two matching procedures are the same. Because the intermediate-expansion procedure meets the sufficient (and hence necessary) requirements, it can be concluded that the inspection procedure meets the necessary requirements for this problem.

Matching by inspection.- An examination of the inner expansion for $\tilde{r} >> \tilde{y}_2$ and the outer expansion for $\bar{r} << 1$ shows that the undetermined functions of x in those expansions can be related as

$$g_\delta + g_{2,1} + H = G_1$$

$$A = F_e F_e' + \frac{\gamma + 1}{2} a^2 f' f''$$

$$B = f$$

$$g_2 = G_3$$

$$C = H$$

Consequently, the inner expansion for $\tilde{r} >> \tilde{y}_2$ and the outer expansion for $\bar{r} << 1$ can be written as

$$\varphi(x,r,\theta) = U_\infty \ell \left(\lambda \sin \alpha f(\bar{x}) \frac{\sin \theta}{\tilde{r}} - \delta^2 \log_e\left(\frac{1}{\lambda\nu}\right) F_e(\bar{x}) F_e'(\bar{x}) + \delta^2 \left[G_1(\bar{x}) + F_e(\bar{x}) F_e'(\bar{x}) \log_e \tilde{r} \right] - \lambda^4 \sin^2 \alpha \log_e^2\left(\frac{1}{\lambda\nu}\right) \frac{\gamma + 1}{4} f'(\bar{x}) f''(\bar{x}) \right.$$

$$- \lambda^4 \sin^2 \alpha \log_e\left(\frac{1}{\lambda\nu}\right) H(\bar{x}) + \lambda^4 \sin^2 \alpha \left\{ G_3(\bar{x}) + H(\bar{x}) \log_e \tilde{r} + \frac{\gamma + 1}{4} f'(\bar{x}) f''(\bar{x}) \log_e^2 \tilde{r} - \frac{f'(\bar{x})}{2} \left[\frac{1}{\lambda^2} - \frac{\gamma + 1}{4} f''(\bar{x}) \right. \right.$$

$$\left. \left. \left. - \frac{f(\bar{x})}{2\lambda^2 \bar{r}^2} \right] \cos 2\theta + \frac{f(\bar{x}) f'(\bar{x})}{4\lambda^2 \bar{r}^2} \right\} + \ldots \right) \tag{67}$$

and

$$\varphi(x,r,\theta) = U_\infty \ell \left(\nu^2 \left\{ G_1(\bar{x}) + \left[F_e(\bar{x})\, F_e'(\bar{x}) + \frac{\gamma+1}{2} a^2 f'(\bar{x})\, f''(\bar{x}) \right] \log_e \bar{r} \right\} \right.$$

$$+ \frac{\nu^2 a}{\sqrt{\log_e \frac{1}{\lambda\nu}}} \left(f(\bar{x}) \frac{\sin\theta}{\tilde{r}} + \cdots \right) + \frac{\nu^2 a^2}{\log_e \frac{1}{\lambda\nu}} \left\{ G_3(\bar{x}) + H(\bar{x}) \log_e \bar{r} \right.$$

$$\left. \left. + \frac{\gamma+1}{4} f'(\bar{x})\, f''(\bar{x}) \log_e^2 \bar{r} - \frac{f'(\bar{x})}{2} \left[\frac{1}{\lambda^2} - \frac{\gamma+1}{4} f''(\bar{x}) \right] \cos 2\theta + \cdots \right\} + \cdots \right) \qquad (68)$$

respectively. The functions G_1 and G_3 cannot be determined with this method. Methods for determining these functions will be discussed subsequently.

If the effects of lift and thickness are comparable in the outer region, the parameter ν in equations (67) and (68) can be equated to the equivalent thickness δ and the angle of attack α can be related to ν, and hence δ, by equation (54). If the effects of lift are dominant in the outer region, the parameter ν is related to α by equation (54) (the order-one constant a can be given a value of one) and the thickness terms in equations (67) and (68) can be considered to be small.

It should be noted that regardless of whether the flow in the outer region is governed by thickness or lift or both, the lowest order term in the outer region is a source term (a term which varies as $\log_e \bar{r}$). It can be seen from equation (68) that even when lift is dominant in the outer region, the dipole term (the term which varies as $\frac{1}{\bar{r}} \sin\theta$) is of secondary importance compared with the source term. From equation (68) it is seen also that the source strength is of the form

$$\frac{1}{\pi} S_a' = \left[F_e^2 + \frac{\gamma+1}{2} a^2 (f')^2 \right]' \qquad (69)$$

when the effects of lift and thickness are comparable in the outer region and of the form

$$\frac{1}{\pi} S_a' = \frac{\gamma+1}{2} \left[(f')^2 \right]' \qquad (70)$$

when the effects of lift are dominant. (For this case the constant a is equated to one, as discussed previously.) The quantity S_a' is the apparent nondimensional rate of change in the x-direction of the cross-sectional area of the lifting configuration. It is well known, of course, that when the effects of thickness are dominant in the outer region, the source strength is of the form

$$\frac{1}{\pi} S_a' = \left(F_e^2\right)' \tag{71}$$

It should be noted that the function $f(x)$ is the x-distribution of lift for the configuration and that the terms in equations (69) and (70) which depend on f provide the thickness-like flow due to lift which was anticipated intuitively and depicted in figure 2.

Matching with intermediate expansion.- Kaplun and Lagerstrom (ref. 12) have established a procedure for matching expansions term by term. It is assumed in this procedure that matching can be performed only in regions where both expansions are valid. An examination of expansions (eqs. (67) and (68)) shows that these expansions cannot have a common region of validity since the leading term of the former contains a dipole and no source and the leading term of the latter contains a source and no dipole. Consequently, the procedure of reference 12 cannot be used to match expansions (eqs. (67) and (68)) directly.

Although the use of the Kaplun and Lagerstrom procedure is not necessary in order for a matching of expansions to be valid, it is sufficient in order to establish validity. There are two ways in which this procedure can be applied to the present problem. One approach is to modify the definition of either the inner or the outer radial variable or both so that the expansions in terms of these variables have a common region of validity. The second approach is to introduce an intermediate variable in such a manner that the region of validity of the intermediate expansion overlaps the regions of validity of the inner and outer expansions. Actually, the distinction may be somewhat academic since the intermediate variable may be simply a generalization of the inner or outer variable. However, from a procedural point of view, it is the second approach which is used in this report.

The intermediate variables $\hat{x}$ and $\hat{r}$ are chosen to be

$$\left.\begin{aligned} \hat{x} &= \tilde{x} = \overline{x} \\ \hat{r} &= \lambda\nu\tilde{r} \log_e^N\left(\frac{1}{\lambda\nu}\right) = \overline{r} \log_e^N\left(\frac{1}{\lambda\nu}\right) \end{aligned}\right\} \tag{72}$$

where

$$0 \leqq N < \infty$$

Note that $\hat{r}$ coincides with $\overline{r}$ for $N = 0$ and that the ratio $\hat{r}/\tilde{r}$ increases monotonically with N but is always small. The expansion in terms of $\hat{r}$ should coincide with the outer expansion for $N = 0$ and should match term by term with the inner expansion for large values of N. The intermediate expansion is written as

$$\varphi = U_\infty \ell \left[\mu_1 \chi_1(\hat{x},\hat{r},\theta) + \mu_2 \chi_2(\hat{x},\hat{r},\theta) + \ldots \right] \tag{73}$$

From an inspection of the inner expansion (eq. (67)) written in terms of $\hat{r}$ and the governing equation (eq. (7)) written in terms of the intermediate expansion (eq. (73)) and $\hat{r}$, it can be shown that the first eight gage functions are written in terms of ν, λ, and N as

$$\left.\begin{aligned}
\mu_1 &= \nu^2 a \left(\log_e \frac{1}{\lambda\nu}\right)^{N-1/2} \\
\mu_2 &= \nu^2 \log_e \left(\log_e \frac{1}{\lambda\nu}\right)^{N} \\
\mu_3 &= \nu^2 \\
\mu_4 &= \frac{\nu^2 a^2 \log_e^2 \left(\log_e \frac{1}{\lambda\nu}\right)^{N}}{\log_e \frac{1}{\lambda\nu}} \\
\mu_5 &= \frac{\nu^2 a^2 \log_e \left(\log_e \frac{1}{\lambda\nu}\right)^{N}}{\log_e \frac{1}{\lambda\nu}} \\
\mu_6 &= \frac{\nu^2 a^2}{\log_e \frac{1}{\lambda\nu}} \\
\mu_7 &= \frac{\nu^2 a \log_e \left(\log_e \frac{1}{\lambda\nu}\right)^{N}}{\left(\log_e \frac{1}{\lambda\nu}\right)^{N+1/2}} \\
\mu_8 &= \frac{\nu^2 a}{\left(\log_e \frac{1}{\lambda\nu}\right)^{N+1/2}}
\end{aligned}\right\} \tag{74}$$

For $N > \frac{1}{2}$ the orders of magnitude of these gage functions increase monotonically with the index. For $N < \frac{1}{2}$, these gage functions are ordered as

$$\mu_2 > \mu_3 > \mu_1 > \mu_7 > \mu_8 > \mu_4 > \mu_5 > \mu_6 \tag{75}$$

From equations (7), (72), (73), and (74), it can be shown that the intermediate potentials χ_1 to χ_5 are governed by the two-dimensional Laplace equation in the cross-flow plane and that the potentials χ_6, χ_7, and χ_8 are governed by the Poisson equations

$$\hat{\nabla}_2^2 \chi_6 = (\gamma + 1)\chi_1' \chi_1'' + 2\left(\frac{\partial \chi_1'}{\partial \hat{r}} \sin\theta + \frac{1}{\hat{r}} \frac{\partial \chi_1'}{\partial \theta} \cos\theta\right) \tag{76}$$

$$\hat{\nabla}_2^2 \chi_7 = (\gamma + 1)\left(\chi_1' \chi_2'\right)' + 2\left(\frac{\partial \chi_2'}{\partial \hat{r}} \sin\theta + \frac{1}{\hat{r}} \frac{\partial \chi_2'}{\partial \theta} \cos\theta\right) \tag{77}$$

$$\hat{\nabla}_2^2 \chi_8 = (\gamma + 1)\left(\chi_1' \chi_3'\right)' + 2\left(\frac{\partial \chi_3'}{\partial \hat{r}} \sin\theta + \frac{1}{\hat{r}} \frac{\partial \chi_3'}{\partial \theta} \cos\theta\right) - K\chi_1'' \tag{78}$$

It should be noted that the governing equations of the intermediate potentials are all independent of the parameter N. Consequently, the solutions are independent of N also. Higher order gage functions and the governing equations for higher order potentials can be obtained in a straightforward manner.

When the Laplace equations governing the potentials χ_1 to χ_5 and equations (76), (77), and (78) for χ_6, χ_7, and χ_8, respectively, are integrated, and the resulting intermediate expansion with $N \geq \frac{1}{2}$ is matched term by term with inner expansion in the manner outlined by Van Dyke (ref. 13), it is found that the solutions for the intermediate potentials are written as

$$\chi_1 = f(\hat{x}) \frac{\sin\theta}{\hat{r}} \tag{79a}$$

$$\chi_2 = -\left[F_e(\hat{x})\, F_e'(\hat{x}) + \frac{\gamma + 1}{2} a^2 f'(\hat{x})\, f''(\hat{x})\right] \tag{79b}$$

$$\chi_3 = G_1(\hat{x}) + \left[F_e(\hat{x})\, F_e'(\hat{x}) + \frac{\gamma + 1}{2} a^2 f'(\hat{x})\, f''(\hat{x})\right] \log_e \hat{r} \tag{79c}$$

$$\chi_4 = \frac{\gamma + 1}{4} f'(\hat{x})\, f''(\hat{x}) \tag{79d}$$

$$\chi_5 = -\left[H(\hat{x}) + \frac{\gamma + 1}{2} f'(\hat{x})\, f''(\hat{x}) \log_e \hat{r}\right] \tag{79e}$$

$$\chi_6 = G_3(\hat{x}) + H(\hat{x}) \log_e \hat{r} + \frac{\gamma + 1}{4} f'(\hat{x})\, f''(\hat{x}) \log_e^2 \hat{r} - \frac{f'(\hat{x})}{2}\left[\frac{1}{\lambda^2} - \frac{\gamma + 1}{4} f''(\hat{x})\right] \cos 2\theta \tag{79f}$$

$$\chi_7 = -\frac{\gamma + 1}{2}\left\{f'(\hat{x})\left[F_e(\hat{x})\, F_e'(\hat{x}) + \frac{\gamma + 1}{2} a^2 f'(\hat{x})\, f''(\hat{x})\right]'\right\} \hat{r} \log_e \hat{r} \sin\theta \tag{79g}$$

$$\chi_8 = \left\{\left(F_e F_e' + \frac{\gamma+1}{2} a^2 f' f''\right)' - \frac{K}{2} f'' + \frac{\gamma+1}{4}\left[f'\left(2G_1' - F_e F_e' - \frac{\gamma+1}{2} a^2 f' f''\right)'\right]'\right\} \hat{r} \log_e \hat{r} \sin\theta$$

$$+ \frac{\gamma+1}{4}\left[f'\left(F_e F_e' + \frac{\gamma+1}{2} a^2 f' f''\right)'\right]' \hat{r} \log_e^2 \hat{r} \sin\theta \qquad (79h)$$

Note that the validity of these solutions does not depend on the parameter N and hence the relative orders of magnitude of the intermediate gage functions. It can be shown that for $N < \frac{1}{2}$, the gage functions are ordered as inequalities (eq. (75)) indicate, and the intermediate expansion can be matched term by term with outer expansion (eq. (68)). (See eq. (65) for additional terms in the outer potential Φ_2.) For $N = 0$ the intermediate and outer expansions coincide.

It has been shown that there is an intermediate expansion (eq. (73)) with gage functions and potentials given by equations (74) and (79), respectively, which has a region of validity that overlaps those of the inner and outer expansions. It has also been shown that the results for the inner and outer expansions obtained by use of the intermediate expansion are the same as those obtained by inspection. Consequently, it is concluded that the inspection procedure is adequate for the present problem.

Solution Near Configuration Surface

The solution near the surface of the configuration can now be determined to within an arbitrary additive function of x. This solution is written in terms of inner variables to second order in $\sin\alpha$ and δ as

$$\varphi = U_\infty \ell \left\{\lambda \sin\alpha\, \phi_1(\tilde{x},\tilde{y},\tilde{z}) - \delta^2 \log_e\left(\frac{1}{\lambda\nu}\right) F_e(\tilde{x})\, F_e'(\tilde{x}) + \delta^2\left[G_1(\tilde{x}) + \psi_2(\tilde{x},\tilde{y},\tilde{z})\right]\right.$$

$$- \lambda^4 \sin^2\alpha \log_e^2\left(\frac{1}{\lambda\nu}\right) f'(\tilde{x})\, f''(\tilde{x}) - \lambda^4 \sin^2\alpha \log_e\left(\frac{1}{\lambda\nu}\right) H(\tilde{x}) + \lambda^4 \sin^2\alpha \left[G_3(\tilde{x}) + \phi_{2a}^P(\tilde{x},\tilde{y},\tilde{z})\right.$$

$$\left.\left. + \phi_{2a}^C(\tilde{x},\tilde{y},\tilde{z}) + \phi_{2b}^P(\tilde{x},\tilde{y},\tilde{z}) + \phi_{2b}^C(\tilde{x},\tilde{y},\tilde{z}) + \phi_{2c}^P(\tilde{x},\tilde{y},\tilde{z}) + \phi_{2c}^C(\tilde{x},\tilde{y},\tilde{z}) + \phi_{2d}(\tilde{x},\tilde{y},\tilde{z})\right]\right\} \qquad (80)$$

where ϕ_1 is one of the basic lift potentials discussed in appendixes A and B, f is the related dipole strength distribution, F_e is the equivalent thickness distribution given by equation (31), ψ is the near-field thickness function given by equation (30), H is the secondary second-order outer-region source-strength distribution given by equation (51), ϕ_{2a}^P, ϕ_{2b}^P, and ϕ_{2c}^P are the second-order particular solutions given by equations (C11), (C15), and (C20), respectively, ϕ_{2a}^C, ϕ_{2b}^C, and ϕ_{2c}^C are the second-order complementary

solutions given by equations (C13), (C18), and (C23), respectively, and ϕ_{2d} is the solution given by equation (48). It should be noted that the presence of the body has been ignored in the derivation of the expressions for ϕ_{2a}^{P}, ϕ_{2b}^{P}, ϕ_{2c}^{P}, ϕ_{2a}^{C}, ϕ_{2b}^{C}, ϕ_{2c}^{C}, and ϕ_{2d}. It should also be noted that the function $\delta^2 G_1(\tilde{x}) + \lambda^4 \sin^2 \alpha\, G_3(\tilde{x})$ cannot be determined with the present method. The determination of this function is discussed in the next section.

Equation (80) for the perturbation velocity potential can be used to determine the pressure coefficient at the configuration surface. It is shown in reference 4 that the pressure coefficient in terms of body-oriented cylindrical polar coordinates is

$$C_p = -\frac{2}{U_\infty}\left[\frac{\partial \varphi}{\partial x} + \sin\alpha\left(\sin\theta\,\frac{\partial \varphi}{\partial \tilde{r}} + \frac{\cos\theta}{r}\,\frac{\partial \varphi}{\partial \theta}\right)\right] - \frac{1}{U_\infty^2}\left[\left(\frac{\partial \varphi}{\partial r}\right)^2 + \frac{1}{r^2}\left(\frac{\partial \varphi}{\partial \theta}\right)^2\right]$$

Determination of Additive Function

The solution for transonic flow over a lifting slender configuration has been determined to within an arbitrary additive function of distance along the axis. It has been pointed out previously that this function cannot be determined with the method of matched asymptotic expansions. Consequently, the solution for this function must be obtained with another method.

It should be noted that the method of matched asymptotic expansions can be used to determine the solution for potential flow past a slender body to within an arbitrary function of distance along the axis also. For subsonic and supersonic slender-body flows, which are governed by a linear equation, this function can be determined with the integral equation method. (See ref. 26.) Spreiter and Alksne (ref. 27) and Aoyama and Wu (ref. 28) present approximate methods for determining this function for transonic slender-body flows, which are governed by a nonlinear equation. However, these approximate methods are not, in general, as accurate as required. At present, solutions of sufficient accuracy can be obtained only with numerical methods which treat the full two-variable problem rather than the one-variable problem for the additive function. One such method for treating the transonic slender-body problem is that of Bailey (ref. 29), which is based on the successive line overrelaxation technique developed by Murman and Cole (ref. 30).

The approximate methods of Spreiter and Alksne (ref. 27) and Aoyama and Wu (ref. 28) could be generalized and applied to the present problem of transonic flow past a lifting slender configuration. However, the more accurate approach of solution by numerical integration is preferable. Three-dimensional numerical calculations of transonic flow about wings and wing-body configurations have been made with methods based on that of Murman and Cole. (See ref. 31, for example.) However, because of their three-dimensional nature, these calculations require large amounts of computing time and

computer storage. Rapid two-variable approximate methods for treating the present problem have been developed by Barnwell (ref. 32) and Cheng and Hafez (ref. 25). The approximations used in these methods are based on the theory presented in this report and reference 9. It should be noted that the method of Barnwell can be used in the angle-of-attack range of order $\frac{\delta}{\sqrt{\log_e \frac{1}{\delta}}}$ (δ is the equivalent thickness ratio), and that the method of Cheng and Hafez is restricted to the much smaller angle-of-attack range of order δ^2.

NONSLENDER-CONFIGURATION PROBLEM

Wings are described traditionally as being nonslender if the reduced-span—length ratio $\sqrt{\left|1 - M_\infty^2\right|}\, b/\ell$ is of order one. In this section nonlifting nonslender transonic wing theory is reviewed, the scaling relationships for transonic flow about nonslender lifting configurations are derived, and it is shown that second-order nonslender wing theory is in agreement with sweep theory although first-order theory is not. The agreement between second-order theory and sweep theory holds for both nonlifting and lifting flows.

Nonslender Nonlifting Wing Theory

Messiter (ref. 4) and Cole and Messiter (ref. 11) treat the problem of transonic flow past a nonlifting nonslender wing. This problem is characterized by the parameters

$$\left.\begin{aligned} &\left|M_\infty - 1\right| \ll 1 \\ &\sqrt{\left|1 - M_\infty^2\right|}\,\lambda = O(1) \\ &\frac{t_w}{\ell} \ll 1 \end{aligned}\right\} \tag{81}$$

It can be shown that for transonic flow past nonslender wings, there is no inner region where the governing equation simplifies. As in slender configuration theory, the radial length scale in the outer region is of the form ℓ/ν, and the quantities ν, ϵ_1, and $1 - M_\infty^2$ can be related by equation (13). (The slenderness approximation was not made in obtaining this equation.) It can be seen from equations (13) and (81) that the semi-span b, which is the radial length scale near the configuration, is of the form

$$\frac{b}{\ell} = O\left(\frac{1}{\nu}\right)$$

Consequently, the radial length scales in the inner and outer regions are of the same order and, as a result, the governing equation and scaling relationships for the outer region apply all the way to the configuration surface.

The relationship between the wing thickness-length ratio and the parameters ν, ϵ_1, and $1 - M_\infty^2$ can be determined from the surface boundary condition, which is of the form

$$\frac{w_c(x,y,z_w)}{U_\infty} = O\left(\frac{t_w}{\ell}\right)$$

and the expression for the perturbation velocity component w_c in terms of the perturbation velocity potential, which is

$$w_c = \frac{\partial \varphi}{\partial z} = U_\infty \ell \epsilon_1 \nu \frac{\partial \Phi_1}{\partial \overline{z}} \tag{82}$$

It follows from the boundary condition and equations (13) and (82) that ν and t_w/ℓ can be related as

$$\nu = \left(\frac{t_w}{\ell}\right)^{1/3} \tag{83}$$

The gage function ϵ_1 and the free-stream Mach number M_∞ are given in terms of t_w/ℓ by the equations

$$\epsilon_1 = \frac{1 - M_\infty^2}{K} = \left(\frac{t_w}{\ell}\right)^{2/3} \tag{84}$$

It should be noted that the scaling relationships for transonic nonslender-wing theory are the same as those for transonic two-dimensional theory.

Nonslender Lifting-Wing Theory

Consider the problem where the angle of attack α is small but is much larger than the wing thickness-length ratio t_w/ℓ. The boundary condition at the surface of the wing is of the form

$$\frac{w_c(x,y,z_w)}{U_\infty} = O(\sin \alpha) \tag{85}$$

From equations (13), (82), and (85), it can be seen that ν is related to the angle of attack by the equation

$$\nu = (\sin \alpha)^{1/3} \tag{86}$$

and the gage function ϵ_1 and the free-stream Mach number are given by the equations

$$\epsilon_1 = \frac{1 - M_\infty^2}{K} = (\sin \alpha)^{2/3} \tag{87}$$

If the wing thickness-length ratio t_w/ℓ and the angle of attack α are of the same order of magnitude, these quantities can be related by the equation

$$\sin \alpha = a \frac{t_w}{\ell} \tag{88}$$

where a is an order-one constant, and the quantities ν, ϵ_1, and M_∞ can be evaluated with either equations (83) and (84) or (86) and (87).

It was shown in the previous section that the scaling for the outer region applies all the way to the wing surface for nonslender wings and that, as a result, the wing semispan-length ratio λ varies as $1/\nu$. Consequently, for lift-dominated and thickness-dominated nonslender flows, λ is scaled as

$$\lambda = \frac{C}{(\sin \alpha)^{1/3}} \qquad (C = O(1)) \tag{89a}$$

and

$$\lambda = \frac{C}{(t_w/\ell)^{1/3}} \qquad (C = O(1)) \tag{89b}$$

respectively. When $\sin \alpha$ and t_w/ℓ are related by equation (88), both of these equations apply.

It can be shown from equations (7), (9), (10), (83), (84), and (88) that when the effects of lift and thickness are comparable, the outer potential Φ_1 for nonslender flow is governed by equation (59).

Approximate Governing Equation for Nonslender-Configuration Problem

It has been observed by Lomax, Bailey, and Ballhaus (ref. 31) that equation (59) is not adequate for treating flow over swept wings in that the conservation form of this equation does not lead to the same inviscid shock-jump condition for the pressure for flow past an infinite swept wing as obtained from simple sweep theory. In reference 31 it is shown that the proper shock-jump condition for an infinite swept wing can be obtained if several terms are added to the governing equation. It can be shown that all of these additional terms are in the second-order approximation to the governing equation for φ. It is probable that other second-order terms should be included since the terms added in reference 31 were chosen for a special case.

The governing equation for the second-order potential Φ_2 in the outer expansion (eq. (10)) for φ for a nonslender wing has been derived by Messiter (ref. 4). This equation can be written as

$$K\Phi_2'' + \bar{\nabla}_2^2\Phi_2 = (\gamma + 1)\left(\Phi_1'\Phi_2'\right)' + 2\frac{\partial\Phi_1}{\partial\bar{y}}\frac{\partial\Phi_1'}{\partial\bar{y}} + 2\frac{\partial\Phi_1}{\partial\bar{z}}\frac{\partial\Phi_1'}{\partial\bar{z}} - (\gamma + 1)K\Phi_1'\Phi_1''$$

$$+ (\gamma - 1)\Phi_1'\bar{\nabla}_2^2\Phi_1 + \frac{\gamma + 1}{2}\left(\Phi_1'\right)^2\Phi_1'' \tag{90}$$

The gage function ϵ_2 was found to be

$$\epsilon_2 = \nu^4 \tag{91}$$

The value of the quantity ν in equation (91) is given by equations (83), (86), or both. Let the velocity potential be approximated by the first two terms in the outer expansion (eq. (10)) so that

$$\varphi \approx \epsilon_1\Phi_1 + \epsilon_2\Phi_2 \tag{92}$$

It can be shown from equations (13), (59), (84), (90), (91), and (92) that the governing equation for the second-order approximation to φ is

$$\left(1 - M_\infty^2\right)\frac{\partial^2\varphi}{\partial x^2} + \nabla_2^2\varphi = (\gamma + 1)M_\infty^2\frac{\partial\varphi}{\partial x}\frac{\partial^2\varphi}{\partial x^2} + 2\frac{\partial\varphi}{\partial y}\frac{\partial^2\varphi}{\partial x\,\partial y} + 2\frac{\partial\varphi}{\partial z}\frac{\partial^2\varphi}{\partial x\,\partial z}$$

$$+ (\gamma - 1)\frac{\partial\varphi}{\partial x}\nabla_2^2\varphi + \frac{\gamma + 1}{2}\left(\frac{\partial\varphi}{\partial x}\right)^2\frac{\partial^2\varphi}{\partial x^2} \tag{93}$$

It is clear that the terms on the left and the first term on the right are those obtained from the first-order equation. The second-order terms which were added in reference 31 are the terms on the right which involve derivatives with respect to y.

COMPARISON OF SLENDER- AND NONSLENDER-WING THEORY

In this section the Mach number range and flow-field structure for slender-wing and nonslender-wing flows are compared, and the Mach number range and flow-field structure for flows which exhibit both slender-wing and nonslender-wing characteristics are determined.

Mach Number Range and Structure of Slender-Wing Flows

For purposes of comparison, configurations composed of wings alone are considered. It has been shown that if slender-wing theory is applicable, the velocity potential in the outer region can be written to lowest order as

$$\varphi = U_\infty \ell \delta^2 \, \Phi_1(\bar{x},\bar{y},\bar{z}) \tag{94}$$

It can be shown from equations (1) and (3) that the equivalent-body thickness δ can be written as

$$\delta^2 = \frac{1}{C_w} \lambda \frac{t_w}{\ell} \qquad \left(C_w = O(1)\right) \tag{95}$$

where, for slender-wing theory,

$$\lambda = \frac{b}{\ell} = O(1)$$

Since the parameter λ can be associated with the aspect ratio, the wings under consideration have aspect ratios of order one. It can be shown from equations (94) and (95) that the velocity perturbations in the outer region can be written as

$$\left.\begin{aligned} \frac{u}{U_\infty} &= \delta^2 \frac{\partial \Phi_1}{\partial \bar{x}} = O\left(\frac{t_w}{\ell}\right) \\ \frac{v_c}{U_\infty} &= \delta^3 \frac{\partial \Phi_1}{\partial \bar{y}} = O\left[\left(\frac{t_w}{\ell}\right)^{3/2}\right] \\ \frac{w_c}{U_\infty} &= O\left[\left(\frac{t_w}{\ell}\right)^{3/2}\right] \end{aligned}\right\} \tag{96}$$

These perturbations are found in a region of the cross-flow plane bounded on the outside by a radius r of the order

$$\frac{r}{\ell} = O\left(\frac{1}{\delta}\right) = O\left[\left(\frac{t_w}{\ell}\right)^{-1/2}\right] \tag{97}$$

and on the inside by a radius which satisfies the inequality

$$r \gg b = \lambda \ell$$

Inside this region the perturbations are obtained from the inner expansion and, as a result, are larger. The governing equation in the bounded outer region where equations (96) apply is of mixed elliptic-hyperbolic type. In the inner region the governing equation is parabolic and in the far field beyond the bounded outer region the equation is elliptic if M_∞ is less than 1 and hyperbolic if M_∞ is greater than 1. The Mach number range in which slender-wing theory applies is

$$M_\infty = 1 + K\delta^2 = 1 + O\left(\frac{t_w}{\ell}\right) \tag{98}$$

Mach Number Range and Structure of Nonslender-Wing Flows

It has been shown that the velocity potential for nonslender-wing theory can be written as

$$\varphi = U_\infty \ell \left(\frac{t_w}{\ell}\right)^{2/3} \Phi_1(\bar{x},\bar{y},\bar{z}) \tag{99}$$

and that λ is of the form

$$\lambda = \frac{b}{\ell} = \frac{C}{\sqrt[3]{t_w/\ell}} \qquad (C = O(1)) \tag{100}$$

Consequently, nonslender-wing theory applies to large-aspect-ratio wings. From equation (99) it can be shown that the velocity perturbations are of the form

$$\left.\begin{aligned} \frac{u}{U_\infty} &= \left(\frac{t_w}{\ell}\right)^{2/3} \frac{\partial \Phi_1}{\partial \bar{x}} = O\left[\left(\frac{t_w}{\ell}\right)^{2/3}\right] \\ \frac{v_c}{U_\infty} &= \frac{t_w}{\ell} \frac{\partial \Phi_1}{\partial \bar{y}} = O\left(\frac{t_w}{\ell}\right) \\ \frac{w_c}{U_\infty} &= O\left(\frac{t_w}{\ell}\right) \end{aligned}\right\} \tag{101}$$

These perturbations are applicable in a region which extends above and beneath the wing to a distance of the order

$$\frac{|z|}{\ell} = O\left[\left(\frac{t_w}{\ell}\right)^{-1/3}\right] \tag{102}$$

The governing equation is of mixed elliptic-hyperbolic type in this region and of elliptic or hyperbolic type in the far field. The Mach number range in which nonslender-wing theory applies is

$$M_\infty = 1 + K\left(\frac{t_w}{\ell}\right)^{2/3} = 1 + O\left[\left(\frac{t_w}{\ell}\right)^{2/3}\right] \tag{103}$$

It can be seen from equations (96) and (101) that for wings with a given thickness ratio, the velocity perturbations obtained from nonslender-wing theory, which applies to wings of large aspect ratio, are larger than those obtained from slender-wing theory, which applies to wings with aspect ratios of order one or less. From equations (97) and (102) it can be determined that the radial extent of the slender-wing perturbations is larger, and from equations (98) and (103) it is seen that the Mach number range in which the nonslender-wing perturbations occur is larger.

Flows Exhibiting Both Slender-Wing and Nonslender-Wing Characteristics

It can be shown that slender- and nonslender-wing theory are both applicable to flow fields about large aspect ratio swept wings if M_∞ is close enough to 1. Such a wing is shown in figure 6. The quantities L, b, and ℓ are the total length, semispan, and chord of the wing. It is assumed that

$$\Lambda = \frac{b}{L} = O(1)$$

$$\lambda = \frac{b}{\ell} >> 1$$

If both theories apply to the same flow field, nonslender-wing theory applies close to the wing where the characteristic length scale in the x-direction is the chord ℓ, and slender-wing theory applies at large distances from the configuration where the length scale in the x-direction is the total length L.

In the region close to the wing where nonslender-wing theory applies, the velocity potential is given by equation (99) and the perturbation velocities satisfy equations (101). These equations pertain in the Mach number range given by equation (103) and in a region which extends above and beneath the wing a distance of the order of the length scale $\ell(t_w/\ell)^{-1/3}$. This region of the cross-flow plane is depicted in the cross section in figure 6. The governing equations in this region are of mixed elliptic-hyperbolic type. The aspect ratio of the wing is given by equation (100). It follows from equation (100) that the chord-length and thickness-length ratios are

$$\frac{\ell}{L} = \frac{\ell}{b}\frac{b}{L} = \frac{\Lambda}{C}\left(\frac{t_w}{\ell}\right)^{1/3}$$

$$\frac{t_w}{L} = \frac{t_w}{\ell}\frac{\ell}{L} = \frac{\Lambda}{C}\left(\frac{t_w}{\ell}\right)^{4/3}$$

From figure 6(a) it can be seen that the equivalent thickness-length ratio is given by the equation

$$\delta^2 = \frac{t^2}{L^2} = \frac{t_w}{L}\frac{b}{L}\frac{\ell}{L} = \Lambda\frac{t_w}{L}\frac{\ell}{L} = \frac{\Lambda^3}{C^2}\left(\frac{t_w}{\ell}\right)^{5/3}$$

Slender-wing theory applies if the Mach number is in the range

$$M_\infty = 1 + O(\delta^2) = 1 + O\left[\left(\frac{t_w}{\ell}\right)^{5/3}\right] \tag{104}$$

The velocity potential in the outer region (the region at large radial distances from the body) is written as

$$\varphi = U_\infty L\delta^2\,\Phi_1(\bar{x},\bar{y},\bar{z}) = U_\infty L\frac{\Lambda^3}{C^2}\left(\frac{t_w}{\ell}\right)^{5/3}\Phi_1(\bar{x},\bar{y},\bar{z})$$

where, in this case, the outer variables $\bar{x}$, $\bar{y}$, and $\bar{z}$ are written as

$$\bar{x} = \frac{x}{L}$$

$$\bar{y} = \delta\frac{y}{L} = \frac{\Lambda^{3/2}}{C}\left(\frac{t_w}{\ell}\right)^{5/6}\frac{y}{L}$$

$$\bar{z} = \frac{\Lambda^{3/2}}{C}\left(\frac{t_w}{\ell}\right)^{5/6}\frac{z}{L}$$

It follows that the velocity perturbations in the outer region are of the order

$$\frac{u}{U_\infty} = O\left[\left(\frac{t_w}{\ell}\right)^{5/3}\right]$$

$$\frac{v_c}{U_\infty} = O\left[\left(\frac{t_w}{\ell}\right)^{5/2}\right]$$

$$\frac{w_c}{U_\infty} = O\left[\left(\frac{t_w}{\ell}\right)^{5/2}\right]$$

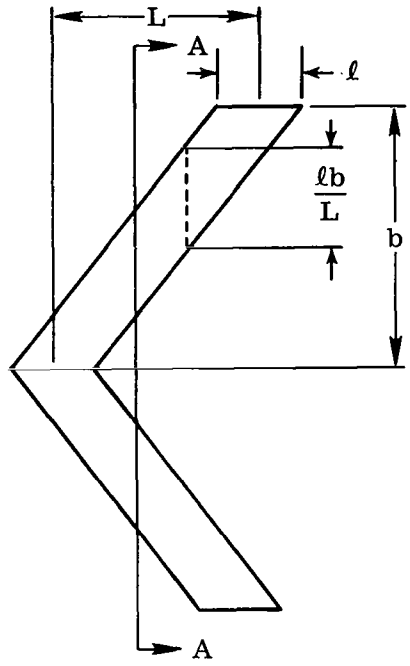

(a) Wing planform.

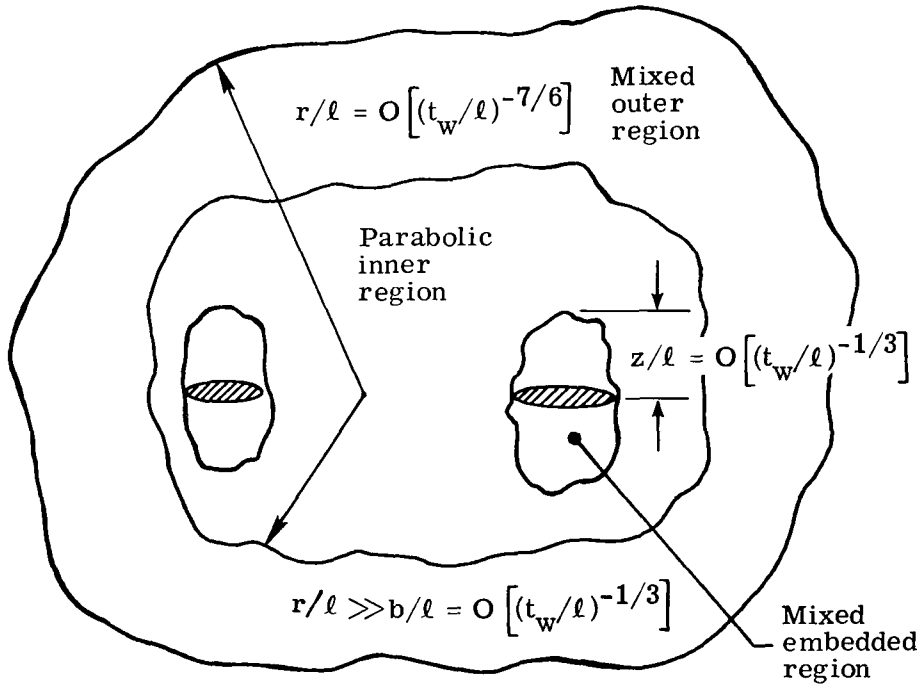

(b) Cross section A-A.

Figure 6.- Large-aspect-ratio wing to which both slender- and nonslender-wing theory apply for $M_\infty = 1 + O\left[\left(\frac{t_w}{\ell}\right)^{5/3}\right]$.

As shown in figure 6(b), the outer region is bounded on the outside by a radius of the order

$$\frac{r}{\ell} = O\left(\frac{L}{\ell\delta}\right) = O\left[\left(\frac{t_w}{\ell}\right)^{-7/6}\right]$$

and on the inside by a radius of the order

$$\frac{r}{\ell} >> \frac{b}{\ell} = \frac{\Lambda L}{\ell} = O\left[\left(\frac{t_w}{\ell}\right)^{-1/3}\right] \tag{105}$$

According to slender-wing theory, the governing equation is of mixed and parabolic type in the outer and inner regions, respectively, and of either elliptic or hyperbolic type in the far field beyond the outer region. It can be seen from equation (102) and inequality (105) that the mixed flow region near the wing predicted by nonslender-wing theory is embedded in the parabolic inner region predicted by slender-wing theory if the Mach number falls within the range given by equation (104).

CONCLUDING REMARKS

A solution has been obtained for the perturbation velocity potential for transonic flow past lifting configurations with span-length ratios of order one. This solution pertains to configurations for which the reduced span-length ratio (the product of the span-length ratio and the quantity $\sqrt{|1 - M_\infty^2|}$ where M_∞ is the free-stream Mach number) is small. The angles of attack which are considered are small but are large enough to insure that the effects of lift are either dominant or comparable to the effects of thickness in the outer region. The analysis was performed with the method of matched asymptotic expansions.

It is shown that the lowest order effect of lift in the outer region is in the form of a source, and that the doublet effect is of secondary importance in this region. This finding pertains both when the effects of lift are comparable with those of thickness and when the effects of lift are dominant. As a result of the source flow due to lift, streamlines are deflected outward more than they would be by thickness effects alone.

A short study is made of the flow about lifting nonslender configurations (configurations with reduced span-length ratios of order one). The order of magnitude of the velocity perturbations is established, and it is shown that second-order nonslender-wing theory is in agreement with sweep theory. The results of slender- and nonslender-wing theory are compared, and the Mach number range and general flow-field structure of flows exhibiting both slender and nonslender characteristics are determined.

Langley Research Center,
National Aeronautics and Space Administration,
Hampton, Va., April 11, 1975.

APPENDIX A

EXISTING CROSS-FLOW SOLUTIONS FOR WING-BODY CONFIGURATIONS

As discussed in the text, solutions have been obtained for the cross-flow velocity potentials for the three wing-body configurations depicted in figure 5. The purpose of this appendix is to review these solutions and to determine the asymptotic forms at large distances from the configurations.

Attached Leading-Edge Flow Past Configurations With Swept Leading Edges

General solution.- A cross section of the wing-body configuration is shown in figure 7. The solution for attached leading-edge flow past this configuration was obtained

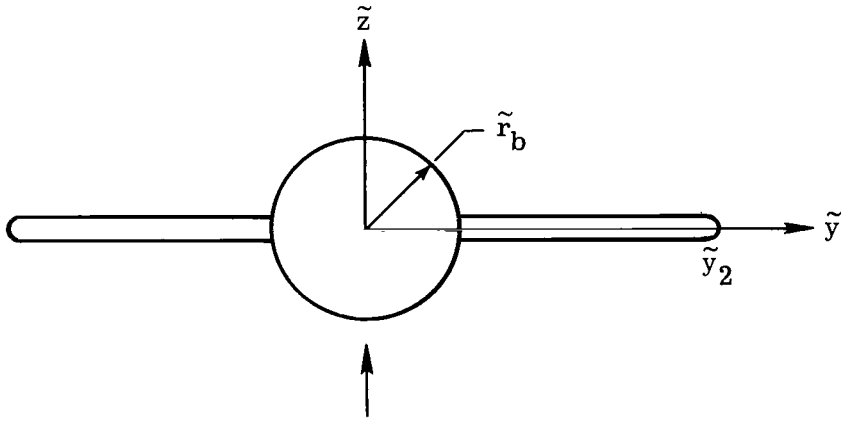

Figure 7.- Cross section of configuration composed of circular body and flat-plate wing.

by Spreiter (ref. 15) and Ward (ref. 16). Let the complex variable in the cross-flow plane be

$$X = \tilde{y} + i\tilde{z}$$

The complex perturbation potential for this problem is written as

$$W(\tilde{x},X) = i\left[X - Y(\tilde{x},X)\right] \tag{A1}$$

where

$$Y(\tilde{x},X) = \sqrt{\left(X + \frac{\tilde{r}_b^2}{X}\right)^2 - \left(\tilde{y}_2 + \frac{\tilde{r}_b^2}{\tilde{y}_2}\right)^2} \tag{A2}$$

The cross-flow perturbation velocity potential is

$$\phi_1(\tilde{x},\tilde{r},\theta) = \mathrm{Re}\left[W(\tilde{x},X)\right]$$

$$= \pm\frac{\sqrt{2}}{2}\left\{-\left(1+\frac{\tilde{r}_b^4}{\tilde{r}^4}\right)\tilde{r}^2\cos 2\theta + \tilde{y}_2^2\left(1+\frac{\tilde{r}_b^4}{\tilde{y}_2^4}\right) + \left[\tilde{r}^4\left(1+\frac{\tilde{r}_b^4}{\tilde{r}^4}\right)^2 + 4\tilde{r}_b^4\cos^2 2\theta\right.\right.$$

$$\left.\left. + \tilde{y}_2^4\left(1+\frac{\tilde{r}_b^4}{\tilde{y}_2^4}\right)^2 - 2\tilde{y}_2^2\left(1+\frac{\tilde{r}_b^4}{\tilde{y}_2^4}\right)\left(1+\frac{\tilde{r}_b^4}{\tilde{r}^4}\right)\tilde{r}^2\cos 2\theta\right]^{1/2}\right\}^{1/2} - \tilde{r}\sin\theta$$

where the relation

$$X = \tilde{r}e^{i\theta}$$

has been used.

Solution far from configuration.- For large values of $\tilde{r}$, equation (A1) can be written as

$$W(\tilde{x},X) = iX\left\{1 - \left[1 - \frac{1}{X^2}\left(\tilde{y}_2^2 + \frac{\tilde{r}_b^4}{\tilde{y}_2^2}\right) + \frac{\tilde{r}_b^4}{X^4}\right]^{1/2}\right\}$$

$$= \frac{i}{X}\left[\frac{1}{2}\tilde{y}_2^2\left(1+\frac{\tilde{r}_b^4}{\tilde{y}_2^4}\right) - \frac{\tilde{y}_2^4}{8X^2}\left(1-\frac{\tilde{r}_b^4}{\tilde{y}_2^4}\right) + \cdots\right]$$

Thus, the velocity potential for large values of $\tilde{r}$ can be written as

$$\phi_1(\tilde{x},\tilde{r},\theta) = \frac{1}{2}\tilde{y}_2^2\left(1+\frac{\tilde{r}_b^4}{\tilde{y}_2^4}\right)\frac{\sin\theta}{\tilde{r}} \tag{A3}$$

For practical purposes the quantity $\left(\tilde{r}_b/\tilde{y}_2\right)^4$ can be neglected since $\tilde{r}_b$ and $\tilde{y}_2$ are generally of orders δ and 1, respectively. Consequently, the velocity potential for large values of $\tilde{r}$ is

$$\phi_1(\tilde{x},\tilde{r},\theta) \approx \frac{1}{2}\tilde{y}_2^2\frac{\sin\theta}{\tilde{r}} \tag{A4}$$

Separated Leading-Edge Flow Past Configurations With Swept Leading Edges

General solution.- Consider configurations composed of circular bodies and flat-plate wings. The cross-flow solution for nonconical configurations of this type was obtained by Wei, Levinsky, and Su (ref. 18) by use of the method developed by Mangler and Smith (ref. 19) and Smith (ref. 20) for conical flat-plate wings. The physical cross-flow plane and the transform plane are shown in figure 8. The outer part of the vortex

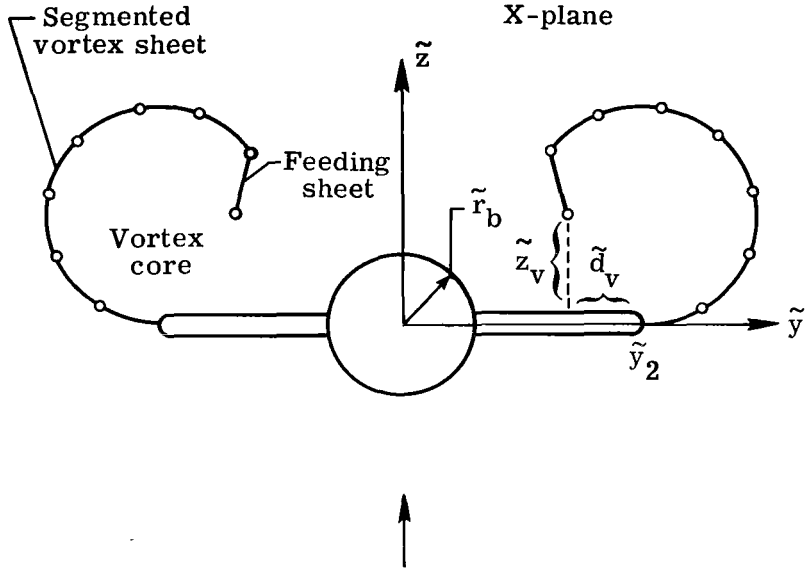

(a) Physical plane.

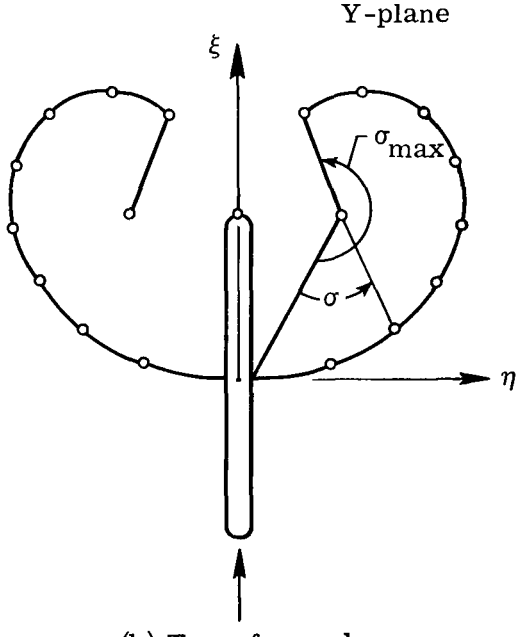

(b) Transform plane.

Figure 8.- Model for separated leading-edge flow.

is approximated with a segmented vortex sheet which emerges from the wing leading edge. The inner part of the vortex sheet is modeled with a vortex core and a feeding sheet which connects the core to the vortex sheet.

The complex perturbation potential for this model is written as

$$W(\tilde{x},X) = i\left(X - Y(\tilde{x},X) - \frac{1}{2\pi}\Gamma_V(\tilde{x})\log_e\left[\frac{Y(\tilde{x},X) - Y(\tilde{x},X_V)}{Y(\tilde{x},X) + Y(\tilde{x},X_V^*)}\right]\right.$$

$$\left. + \frac{1}{2\pi}\int_{\sigma=0}^{\sigma=\sigma_{max}} \frac{d}{d\sigma}\left[\Delta\phi(\tilde{x},\sigma)\right]\log_e\left\{\frac{Y(\tilde{x},X) - Y[\tilde{x},X(\sigma)]}{Y(\tilde{x},X) + Y[\tilde{x},X^*(\sigma)]}\right\} d\sigma\right) \qquad (A5)$$

where the asterisk denotes the complex conjugate, X_V and $X(\sigma)$ are the positions of the vortex core and the centers of the vortex-sheet elements, Γ_V is the strength of the vortex core, and $\Delta\phi$ is the potential jump across the vortex sheet. The values of these quantities are determined from the leading-edge Kutta condition, the condition that the pressure and normal velocity are continuous across the vortex-sheet elements, and the assumption that no force is exerted on the system composed of the vortex core and feeding sheet.

Solution far from configuration.- It can be shown that for angles of attack such that $\sin\alpha << 1$ the term proportional to Γ_V and the integral term in equation (A5) are of order $(\sin\alpha)^c$ where $c \leq 1$ so that equations (A3) and (A4) apply to separated as well as unseparated leading-edge flow. Let $Y(\tilde{x},X_V)$ and $Y(\tilde{x},X_V^*)$ be written as Y_V and Y_V^*, respectively. In the region where $\tilde{r}$ and hence $Y(\tilde{x},X)$ are large, the logarithmic expression for the vortex core in equation (A5) can be written as

$$\log_e\left(\frac{Y - Y_V}{Y + Y_V^*}\right) = \log_e\left(1 - \frac{Y_V}{Y}\right) - \log_e\left(1 + \frac{Y_V^*}{Y}\right) = -2\frac{Re(Y_V)}{Y} \qquad (A6)$$

Assume that the vortex location is

$$X_V = \tilde{y}_2 - \tilde{d}_V + i\tilde{z}_V$$

where $\tilde{d}_V$ and $\tilde{z}_V$ are shown in figure 8. It is reasonable to assume that for small angles of attack, the distance between the vortex core and the wing is of the form

$$\tilde{z}_V = O(\sin\alpha)$$

In fact, Brown and Michael (ref. 33) show that this is the case for their simplified model for conical flow past a delta wing. For d_V, there are two cases of interest. If the vortex core lies near the leading edge of the wing, then $\tilde{d}_V$ is of order $(\sin\alpha)^c$ where $c \leq 1$ $\left(\text{for the Brown and Michael model for conical flow, } c = \frac{2}{3}\right)$. If the vortex core lies inboard of the tip, $\tilde{d}_V$ is of order one.

First consider the case where

$$d_V = O(\sin^c \alpha) \tag{A7}$$

After some algebraic manipulation, it can be shown that Y_V is

$$Y_V \approx \sqrt{2\tilde{y}_2\left(1 - \frac{\tilde{r}_b^4}{\tilde{y}_2^4}\right)\sqrt{\tilde{d}_V^2 + \tilde{z}_V^2}}\, e^{i\beta/2} \tag{A8}$$

where

$$\beta = \pi + \tan^{-1}\left(\frac{-\tilde{z}_V}{\tilde{d}_V}\right) \qquad \left(\tilde{d}_V > 0\right) \tag{A9a}$$

$$\beta = \tan^{-1}\left(\frac{\tilde{z}_V}{\tilde{d}_V}\right) \qquad \left(\tilde{d}_V < 0\right) \tag{A9b}$$

and that

$$\cos\frac{\beta}{2} = \sqrt{\frac{\sqrt{\tilde{d}_V^2 + \tilde{z}_V^2} - \tilde{d}_V}{2\sqrt{\tilde{d}_V^2 + \tilde{z}_V^2}}} \tag{A10}$$

It follows from equations (A8) and (A10) that for large values of $\tilde{r}$, equation (A6) can be written as

$$\log_e\left(\frac{Y - Y_V}{Y + Y_V^*}\right) = 2\sqrt{\tilde{y}_2\left(1 - \frac{\tilde{r}_b^4}{\tilde{y}_2^4}\right)\left(\sqrt{\tilde{d}_V^2 + \tilde{z}_V^2} - \tilde{d}_V\right)}\,\frac{e^{-i\theta}}{\tilde{r}} = \frac{e^{-i\theta}}{\tilde{r}}\, O\left[(\sin\alpha)^{1-\frac{c}{2}}\right]$$

In a similar fashion the terms $\log_e\left[\frac{Y - Y(\sigma)}{Y - Y^*(\sigma)}\right]$ can be shown to be of this order of magnitude also. It can be seen from reference 18 that the leading-edge Kutta condition is written as

$$\Gamma_v \frac{\mathrm{Re}(Y_v)}{|Y_v|^2} - \int_{\sigma=0}^{\sigma=\sigma_{max}} \frac{d}{d\sigma}\left[\Delta\phi(\sigma)\right] \frac{\mathrm{Re}\left[Y(\sigma)\right]}{|Y(\sigma)|^2}\, d\sigma = \pi \tag{A11}$$

From equations (A7), (A8), and (A10), it can be determined that

$$\frac{\mathrm{Re}(Y_v)}{|Y_v|^2} = O\left[(\sin\alpha)^{1-\frac{3c}{2}}\right] \tag{A12}$$

A similar expression applies for $\dfrac{\mathrm{Re}\left[Y(\sigma)\right]}{|Y(\sigma)|^2}$. Since the vortex-core term and the integral term in equation (A11) are generally of the same order of magnitude and do not cancel, it follows that

$$\Gamma_v = O\left[(\sin\alpha)^{\frac{3c}{2}-1}\right]$$

$$\frac{d\Delta\phi}{d\sigma} = O\left[(\sin\alpha)^{\frac{3c}{2}-1}\right]$$

This order-of-magnitude estimate for Γ_v is consistent with the delta-wing results of Brown and Michael (ref. 33) that $c = \frac{2}{3}$ and Γ_v is of order 1. Consequently, the vortex-core term and the integral term in equation (A5) are of the order $(\sin\alpha)^c$ and can be neglected in the first approximation.

Consider the case in which

$$\tilde{d}_v = O(1)$$

and let

$$\tilde{y}_v = \tilde{y}_2 - \tilde{d}_v$$

After considerable manipulation, it is found that

$$Y_v = \sqrt{\tilde{y}_2^2 - \tilde{y}_v^2}\sqrt{1 - \frac{\tilde{r}_b^4}{\tilde{y}_2^2\tilde{y}_v^2}}\, e^{i\beta/2} \tag{A13}$$

where

$$\beta = \pi + \tan^{-1}\left[\frac{-2\tilde{z}_v\tilde{y}_2^2\left(\tilde{y}_v^4 - \tilde{r}_b^4\right)}{\tilde{y}_v\left(\tilde{y}_2^2 - \tilde{y}_v^2\right)\left(\tilde{y}_2^2\tilde{y}_v^2 - \tilde{r}_b^4\right)}\right] \tag{A14}$$

and that

$$\cos\frac{\beta}{2} = \frac{\tilde{z}_v\tilde{y}_2^2\left(\tilde{y}_v^4 - \tilde{r}_b^4\right)}{\tilde{y}_v\left(\tilde{y}_2^2 - \tilde{y}_v^2\right)\left(\tilde{y}_2^2\tilde{y}_v^2 - \tilde{r}_b^4\right)} \tag{A15}$$

From equations (A6), (A13), and (A15), it can be shown that in the first approximation,

$$\log_e\left(\frac{Y - Y_v}{Y + Y_v^*}\right) = \frac{2\left(\tilde{y}_v^4 - \tilde{r}_b^4\right)\tilde{y}_2\tilde{z}_v}{\tilde{y}_v^2\sqrt{\tilde{y}_2^2 - \tilde{y}_v^2}\sqrt{\tilde{y}_2^2\tilde{y}_v^2 - \tilde{r}_b^4}}\frac{e^{-i\theta}}{\tilde{r}} = \frac{e^{-i\theta}}{\tilde{r}}\,O(\sin\alpha)$$

Similarly, the quantities $\log_e\left[\frac{Y - Y(\sigma)}{Y + Y^*(\sigma)}\right]$ can also be shown to be of this order. The magnitude of the core strength Γ_v and the quantities $-d\Delta\phi(\sigma)/d\sigma$ cannot be estimated from equation (A11) in the manner used previously because the orders of magnitude of the distances from the vortex core and vortex-sheet segments to the wing tip vary and the orders of magnitude of the coefficients of the quantities $-d\Delta\phi/d\sigma$ and Γ_v in equation (A11) depend on these distances. However, it is reasonable to assume that the core strength Γ_v and the vortex-sheet segment strengths $-d\Delta\phi/d\sigma$ are of order 1 or smaller. Consequently, the vortex-core term in equation (A5) is of order $\sin\alpha$ or smaller, and the contributions of the various vortex-sheet segments to the integral term vary from order $\sin\alpha$ or smaller near the core to order $(\sin\alpha)^c$ near the tip. These contributions can be neglected in the first approximation.

It is concluded that for separated leading-edge flow, the velocity potential for large values of $\tilde{r}$ is given to lowest order by equation (A3) or (A4), which were derived for attached leading-edge flow. It has been shown that this conclusion applies both when the vortex core is located near the wing tip and when it is located well inboard.

Attached Leading-Edge Flow Past Configurations With Swept Leading and Trailing Edges

General solution.- The derivative $\partial\phi_1/\partial\tilde{x}$ for this problem has been derived by Mirels (ref. 21) and Mangler (ref. 22). The physical plane and the transform plane obtained with the transformation

$$Z = X - \frac{\tilde{r}_b^2}{X} \tag{A16}$$

are shown in figure 9. In the transform plane the derivative $\frac{\partial^2 W}{\partial \tilde{x} \partial Z}$ is written as

$$\frac{\partial^2 W}{\partial \tilde{x} \partial Z} = -i\eta_2 \eta_2' S(\tilde{x}) \left(\frac{Z^2 - \eta_1^2}{Z^2 - \eta_2^2} - \frac{E}{K} \right) \frac{1}{\sqrt{Z^2 - \eta_1^2} \sqrt{Z^2 - \eta_2^2}} \tag{A17}$$

where

$$\eta_1 = \tilde{y}_1 - \frac{\tilde{r}_b^2}{\tilde{y}_1}$$

$$\eta_2 = \tilde{y}_2 - \frac{\tilde{r}_b^2}{\tilde{y}_2}$$

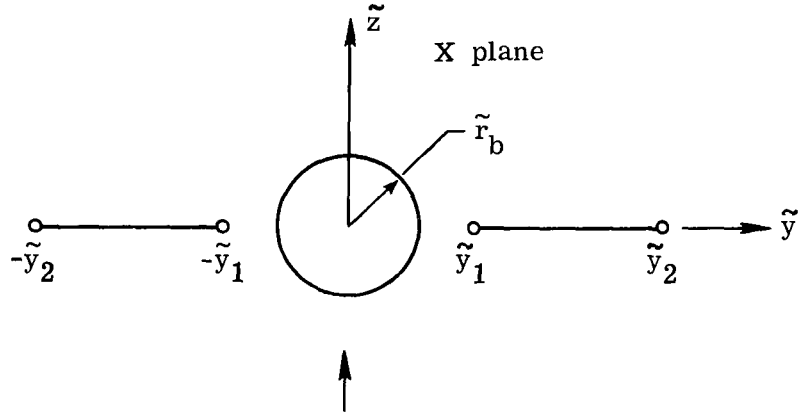

(a) Physical plane.

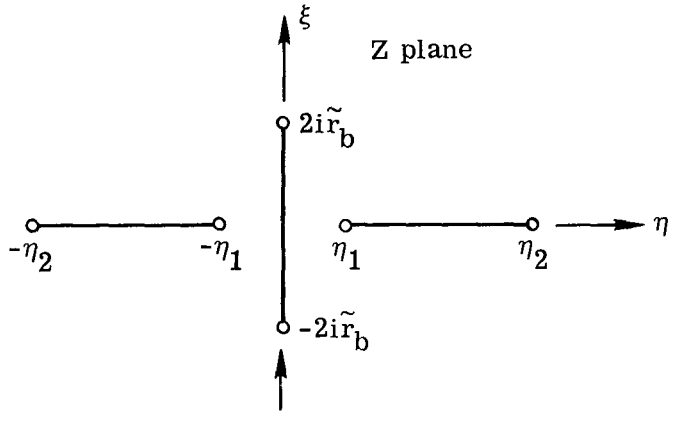

(b) Transform plane.

Figure 9.- Cross-flow planes for attached leading-edge flow past configuration with swept trailing edge.

The function $S(\tilde{x})$ is the function Mirels (ref. 21) developed for enforcing the Kutta condition at the swept trailing edge, and K and E are complete elliptic integrals of the first and second kinds with the modulus

$$k = \sqrt{1 - \frac{\eta_1^2}{\eta_2^2}} \tag{A18}$$

It should be noted that Mirels' S-function is identical to the function H used by Mangler (ref. 22).

Solution far from configuration.- The complex velocity in the physical plane is related to that in the transform plane by the equation

$$\frac{\partial W}{\partial X} = \frac{\partial W}{\partial Z}\frac{\partial Z}{\partial X} = \frac{\partial W}{\partial Z}\left(1 + \frac{\tilde{r}_b^2}{X^2}\right)$$

It follows that the equation for $\frac{\partial^2 W}{\partial \tilde{x}\,\partial X}$ is

$$\frac{\partial^2 W}{\partial \tilde{x}\,\partial X} = \frac{\partial^2 W}{\partial \tilde{x}\,\partial Z}\left(1 + \frac{\tilde{r}_b^2}{X^2}\right) + \frac{2}{X^2}\frac{\partial W}{\partial Z}\tilde{r}_b\tilde{r}_b' \tag{A19}$$

At large distances from the wing and body in the transform plane, equation (A17) can be written as

$$\frac{\partial^2 W}{\partial \tilde{x}\,\partial Z} = -i\eta_2\eta_2'\frac{1}{Z^2}S(\tilde{x})\left(1 - \frac{E}{K}\right)$$

and hence the derivative $\partial W/\partial Z$ is approximately

$$\frac{\partial W}{\partial Z} = i\left[1 - \frac{1}{Z^2}\int S(\tilde{x})\left(1 - \frac{E}{K}\right)\eta_2\eta_2'\,d\tilde{x}\right] = i\left[1 + O\left(\frac{1}{\tilde{r}^2}\right)\right]$$

Thus equation (A19) can be written as

$$\frac{\partial^2 W}{\partial \tilde{x}\,\partial X} = -\frac{i}{X^2}\left[S(\tilde{x})\left(1 - \frac{E}{K}\right)\eta_2\eta_2' - 2\tilde{r}_b\tilde{r}_b'\right]$$

so that the derivative $\partial W/\partial \tilde{x}$ is written as

$$\frac{\partial W}{\partial \tilde{x}} = \frac{i}{X}\left\{\frac{S}{2}\left(1 - \frac{E}{K}\right)\left[\tilde{y}_2^2\left(1 + \frac{\tilde{r}_b^4}{\tilde{y}_2^4}\right)\right]' + 2\left[S\left(1 - \frac{E}{K}\right) - 1\right]\tilde{r}_b\tilde{r}_b'\right\}$$

Therefore, for large values of $\tilde{r}$ the derivative $\partial\phi_1/\partial\tilde{x}$ can be written as

$$\frac{\partial \phi_1}{\partial \tilde{x}} = \frac{S(\tilde{x})}{2}\left(1 - \frac{E}{K}\right)\left[\tilde{y}_2^2\left(1 + \frac{\tilde{r}_b^4}{\tilde{y}_2^4}\right)\right]' \frac{\sin\theta}{\tilde{r}} \tag{A20}$$

where the modulus of E and K is given by equation (A18). The quantities $\tilde{r}_b$ and $\tilde{y}_2$ are of orders δ and 1, respectively, and the quantity $\tilde{y}_1$ varies between orders δ and 1. Consequently, equation (A20) can be written to lowest order as

$$\frac{\partial \phi_1}{\partial \tilde{x}} = S(\tilde{x})\left(1 - \frac{E}{K}\right)\tilde{y}_2\tilde{y}_2' \frac{\sin\theta}{\tilde{r}} \tag{A21}$$

where the modulus of E and K is

$$k = \sqrt{1 - \frac{\tilde{y}_1^2}{\tilde{y}_2^2}} \tag{A22}$$

APPENDIX B

FAR-FIELD APPROXIMATION TO CROSS-FLOW SOLUTIONS FOR CONFIGURATIONS WITH TWISTED AND CAMBERED WINGS

The purpose of this appendix is to develop the far-field approximation to the cross-flow solution for configurations with twisted and cambered wings. The wings which are treated include those with only swept leading edges and those with both swept leading and swept trailing edges. As in the case of flat wings, the approximation for the cross-flow potential ϕ_1 can be determined analytically for wings with swept leading edges only, but only the derivative $\partial\phi_1/\partial\tilde{x}$ can be determined analytically for wings with both swept leading and swept trailing edges. The velocity potential is governed by equation (20), the two-dimensional Laplace equation in the cross-flow plane, and satisfies the boundary conditions (eqs. (18)). Let the potential ϕ_1 be written as the sum

$$\phi_1 = \phi_{1a} + \phi_{1b} \tag{B1}$$

where the potentials ϕ_{1a} and ϕ_{1b} satisfy the boundary conditions

$$\frac{\partial\phi_{1a}\left(\tilde{x},\tilde{r}_b,\theta\right)}{\partial\tilde{r}} = -\sin\theta \tag{B2a}$$

$$\frac{\partial\phi_{1a}(\tilde{x},\tilde{r},0)}{\partial\theta} = -\frac{\partial\phi_{1a}(\tilde{x},\tilde{r},\pi)}{\partial\theta} = -\tilde{r} \tag{B2b}$$

and

$$\frac{\partial\phi_{1b}\left(\tilde{x},\tilde{r}_b,\theta\right)}{\partial\tilde{r}} = 0 \tag{B3a}$$

$$\frac{\partial\phi_{1b}(\tilde{x},\tilde{r},0)}{\partial\theta} = -\frac{\partial\phi_{1b}(\tilde{x},\tilde{r},\pi)}{\partial\theta} = \tilde{r}\, g'(\tilde{x},\tilde{y}) \tag{B3b}$$

respectively. Equations (B2b) and (B3b) apply on the interval $\tilde{y}_2 \geqq \tilde{r} \geqq \tilde{r}_b$ if the wing has no trailing edge and on the interval $\tilde{y}_2 \geqq \tilde{r} \geqq \tilde{y}_1$ if the wing has both leading and trailing edges. If the wing has a trailing edge, equations (B2) and (B3) are supplemented by the equations

$$\frac{\partial\phi_{1a}(\tilde{x},\tilde{r},0)}{\partial\tilde{x}} = \frac{\partial\phi_{1a}(\tilde{x},\tilde{r},\pi)}{\partial\tilde{x}} = 0 \tag{B4}$$

and

$$\frac{\partial \phi_{1b}(\tilde{x},\tilde{r},0)}{\partial \tilde{x}} = \frac{\partial \phi_{1b}(\tilde{x},\tilde{r},\pi)}{\partial \tilde{x}} = 0 \tag{B5}$$

respectively, on the interval $\tilde{y}_1 \geqq \tilde{r} \geqq \tilde{r}_b$.

Configurations With Swept Leading Edges

The solution for the potential ϕ_{1a} which satisfies boundary conditions (eqs. (B2)) for attached leading-edge flow past configurations with unswept trailing edges is derived in the first part of appendix A. The far-field approximation for this potential, which is given to lowest order by equation (A4), is also derived. It should be noted that since equation (A4) does not contain r_b, the use of the lowest order form is equivalent to neglecting the presence of the body. In a similar fashion the far-field approximation for the potential ϕ_{1b} which satisfies boundary conditions (eqs. (B3)) can be approximated with the solution of Klunker and Harder (ref. 23) for attached leading-edge flow past twisted and cambered wings. Let the complex variable in the cross-flow plane for the wing alone be X, and let the boundary condition for the wing be

$$w_c(\tilde{x},\tilde{y},0) = g'(\tilde{x},\tilde{y})$$

$$-\tilde{y}_2(\tilde{x}) \leqq \tilde{y} \leqq \tilde{y}_2(\tilde{x})$$

From equation 1.3 of reference 23 it is seen that the complex velocity in the cross-flow plane of the wing is

$$\frac{\partial W(\tilde{x},X)}{\partial X} = \frac{i}{\pi\sqrt{X^2 - \tilde{y}_2^2(\tilde{x})}} \int_{s=-\tilde{y}_2(\tilde{x})}^{s=\tilde{y}_2(\tilde{x})} \frac{g'(\tilde{x},s)\sqrt{\tilde{y}_2^2(\tilde{x}) - s^2}}{X - s}\, ds \tag{B6}$$

At large distances from the configuration equation (B6) can be written as

$$\frac{\partial W(\tilde{x},X)}{\partial X} = \frac{2i}{\pi X^2} \int_{s=0}^{s=\tilde{y}_2(\tilde{x})} g'(\tilde{x},s)\sqrt{\tilde{y}_2^2(\tilde{x}) - s^2}\, ds \tag{B7}$$

The velocity potential ϕ_{1b} for large values of $\tilde{r}$ can be obtained from equation (B7), and the potential ϕ_{1a} can be obtained from equation (A4). Consequently, at large distances from the configuration, the potential ϕ_1 is written as

$$\phi_1(\tilde{x},\tilde{r},\theta) = \left[\frac{1}{2}\tilde{y}_2^2 - \frac{2}{\pi}\int_{s=\tilde{r}_b}^{s=\tilde{y}_2} g'(\tilde{x},s)\sqrt{\tilde{y}_2^2 - s^2}\,ds\right]\frac{\sin\theta}{\tilde{r}} \tag{B8}$$

Configurations With Swept Leading and Trailing Edges

The solution for the derivative $\partial\phi_{1a}/\partial\tilde{x}$ of the potential which satisfies boundary conditions (eqs. (B2) and (B4)) for attached leading-edge flow past configurations with swept leading and trailing edges is derived in the last part of appendix A. The solution for the derivative $\partial\phi_{1b}/\partial\tilde{x}$ of the potential which satisfies boundary conditions (eqs. (B3) and (B5)) can be approximated with the solution of Klunker and Harder (ref. 23) for flow past twisted and cambered wings. The boundary conditions for the wing treated in reference 23 are written in terms of the notation of this report as

$$w_c(\tilde{x},\tilde{y},0) = g'(\tilde{x},\tilde{y})$$

$$-\tilde{y}_2 \leqq y \leqq -\tilde{y}_1$$

$$\tilde{y}_1 \leqq y \leqq \tilde{y}_2$$

$$u(\tilde{x},\tilde{y},0) = 0$$

$$-\tilde{y}_1 \leqq y \leqq \tilde{y}_1$$

Let the complex variable in the wing cross-flow plane be X. From equation 1.8 of reference 23, it is seen that the $\tilde{x}$ derivative of the complex velocity in the cross-flow plane of the wing is

$$\frac{\partial^2 W(\tilde{x},X)}{\partial\tilde{x}\,\partial X} = \frac{i}{\pi\left(X^2 - \tilde{y}_2^2\right)^{3/2}\sqrt{X^2 - \tilde{y}_1^2}}\left[\int_{s=-\tilde{y}_2}^{s=-\tilde{y}_1} \frac{g''(\tilde{x},s)\left(\tilde{y}_2^2 - s^2\right)^{3/2}\sqrt{s^2 - \tilde{y}_1^2}}{X - s}\,ds\right.$$

$$\left. - \int_{s=\tilde{y}_1}^{s=\tilde{y}_2} \frac{g''(\tilde{x},s)\left(\tilde{y}_2^2 - s^2\right)^{3/2}\sqrt{s^2 - \tilde{y}_1^2}}{X - s}\,ds + A_0(\tilde{x}) + B_0(\tilde{x})\,X^2\right] \tag{B9}$$

where $A_0(\tilde{x})$ and $B_0(\tilde{x})$ are the functions A and B used in reference 23.

At large radial distances from the configuration, equation (B9) can be written as

$$\frac{\partial^2 W}{\partial \tilde{x} \partial X} = \frac{i}{\pi} \frac{B_0(\tilde{x})}{X^2} \tag{B10}$$

The $\tilde{x}$ derivative of ϕ_{1b} can be obtained from equation (B10), and the derivative of ϕ_{1a} can be obtained to lowest order from equation (A20). Consequently, the derivative of ϕ_1 for large values of $\tilde{r}$ can be written as

$$\frac{\partial \phi_1}{\partial \tilde{x}} = \left[S(\tilde{x}) \left(1 - \frac{E}{K} \right) \tilde{y}_2 \tilde{y}_2' - \frac{1}{\pi} B_0(\tilde{x}) \right] \frac{\sin \theta}{\tilde{r}}$$

where the modulus of the complete elliptic integrals E and K is given by equation (A22). A method for determining the function $B_0(x)$ is discussed in section 2 of reference 23.

APPENDIX C

SOLUTIONS FOR SECOND-ORDER LIFT POTENTIALS ϕ_{2a}, ϕ_{2b}, AND ϕ_{2c}

Particular solutions for the potentials ϕ_{2a}, ϕ_{2b}, and ϕ_{2c} are derived in very general form and are given by equations (43), (44), and (46), respectively. The purpose of this appendix is to evaluate these general forms at the configuration surface and to determine the complementary solutions necessary to enforce the boundary conditions.

Cheng and Hafez (ref. 25) have shown that in order for the solution for ϕ_{2a} to exist, the potential ϕ_1 must satisfy a Kutta condition at the leading edge of the wing. In reference 25 solutions are obtained for the potentials ϕ_{2a} and ϕ_{2b} for configurations with wings which are cambered so that this condition is satisfied. In this appendix it is shown that the solutions derived in reference 25 also apply approximately to flow fields where the leading-edge Kutta condition is met by means of leading-edge separation.

As stated in the text, the boundary conditions for the potentials ϕ_{2a}, ϕ_{2b}, and ϕ_{2c} are all homogeneous. In this appendix the body-surface boundary condition is ignored as it was in reference 25. This approximation is permissible since the body surface $\tilde{r}_b$ is of order δ.

Cauchy Representation of ϕ_1 and $\partial\phi_1/\partial\tilde{x}$ for the Leading-Edge Separation Model

The Cauchy representation is used in this appendix as it was in reference 25. The leading-edge separation model which is employed is that used by Mangler and Smith (ref. 19), Smith (ref. 20), Wei, Levinsky, and Su (ref. 18), and others. The complex perturbation potential for this model is given by equation (A5). If the body can be ignored and if the vortex-sheet integration is performed in the physical plane, this equation can be written as

$$W = i\left[X - \sqrt{X^2 - \tilde{y}_2^2} - \frac{\Gamma_v}{2\pi}\log_e\left(\frac{\sqrt{X^2 - \tilde{y}_2^2} - \sqrt{X_v^2 - \tilde{y}_2^2}}{\sqrt{X^2 - \tilde{y}_2^2} + \sqrt{X_v^{*2} - \tilde{y}_2^2}}\right)\right.$$

$$\left. - \frac{1}{2\pi}\int_{s=\tilde{y}_2}^{s=s_{max}} \gamma(\tilde{x},s)\log_e\left(\frac{\sqrt{X^2 - \tilde{y}_2^2} - \sqrt{X_{(s)}^2 - \tilde{y}_2^2}}{\sqrt{X^2 - \tilde{y}_2^2} + \sqrt{X_{(s)}^{*2} - \tilde{y}_2^2}}\right) ds\right] \qquad \text{(C1)}$$

where s is the distance along the wing and vortex sheet from the wing center line, and where the strength of a vortex sheet or wing segment is

$$\gamma(\tilde{x},s) = -\frac{d\Delta\phi(\tilde{x},s)}{ds} \tag{C2}$$

Let a contour be drawn around the system composed of the wing, vortex sheets, feeding sheets, and vortex cores as shown in figure 10. With Cauchy's integral theorem the complex potential W can be written as

$$W = -\frac{i}{\pi}\left\{\int_{s=-s_{max}}^{s=-\tilde{y}_2}\frac{\gamma(\tilde{x},s)}{X(s)-X}\,ds + \int_{s=-\tilde{y}_2}^{s=\tilde{y}_2}\frac{\gamma(\tilde{x},s)}{X(s)-X}\,ds + \int_{s=\tilde{y}_2}^{s=s_{max}}\frac{\gamma(\tilde{x},s)}{X(s)-X}\,ds + \int_{S=-X_v^*}^{S=-X^*(s_{max})}\frac{\Delta W(\tilde{x},S)}{S-X}\,dS + \int_{S=X(s_{max})}^{S=X_v}\frac{\Delta W(\tilde{x},S)}{S-X}\,dS\right.$$

$$\left. + \lim_{\rho\to 0}\left[\rho\int_{\omega=\omega_1}^{\omega=\omega_1-2\pi}\frac{W(\tilde{x},X_v+\rho e^{i\omega})ie^{i\omega}}{X_v+\rho e^{i\omega}-X}\,d\omega + \rho\int_{\omega=\omega_2}^{\omega=\omega_2-2\pi}\frac{W(\tilde{x},-X_v^*+\rho e^{i\omega})ie^{i\omega}}{-X_v^*+\rho e^{i\omega}-X}\,d\omega\right]\right\} \tag{C3}$$

where ΔW is the difference of the complex potential on the inside and outside of the feeding sheet. (See fig. 10.)

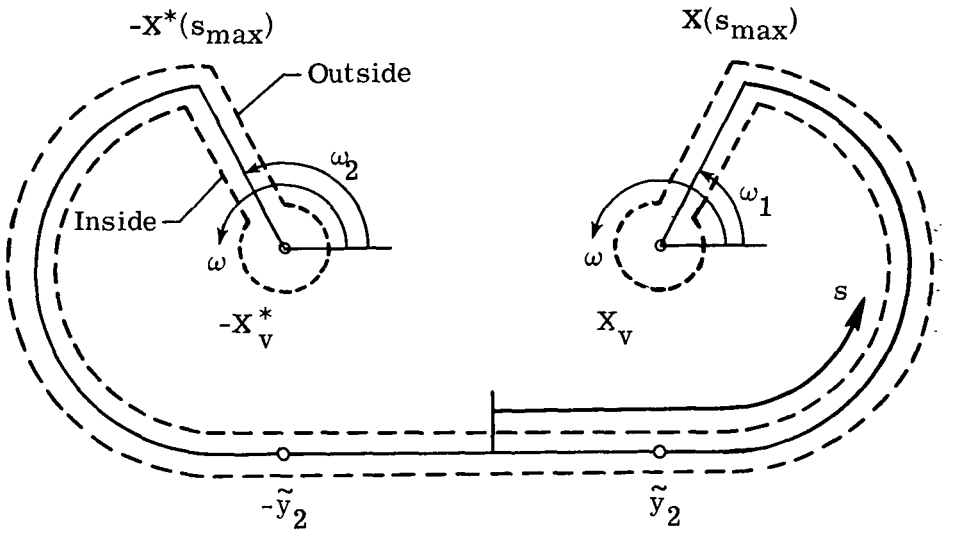

Figure 10.- Contour around wing, vortex sheets, feeding sheets, and vortex cores.

It can be shown that for practical purposes, only the first three terms in equation (C3) need to be retained. Consider the last two terms in equation (C3). With equation (C1) the first of these terms can be written as

$$\lim_{\rho \to 0} \rho \int_{\omega = \omega_1}^{\omega = \omega_1 - 2\pi} \frac{W\left(\tilde{x}, X_v + \rho e^{i\omega}\right) i e^{i\omega}}{X_v + \rho e^{i\omega} - X} \, d\omega$$

$$= \frac{\Gamma_v}{2\pi\left(X_v - X\right)} \lim_{\rho \to 0} \rho \int_{\omega = \omega_1}^{\omega = \omega_1 - 2\pi} \log_e \left[\sqrt{\left(X_v + \rho e^{i\omega}\right)^2 - \tilde{y}_2^2} - \sqrt{X_v^2 - \tilde{y}_2^2} \right] e^{i\omega} \, d\omega \qquad \text{(C4)}$$

where it is assumed that

$$\left| X_v - X \right| >> \rho$$

It can be shown that to the lowest order in ρ

$$\sqrt{\left(X_v + \rho e^{i\omega}\right)^2 - \tilde{y}_2^2} = \sqrt{X_v^2 - \tilde{y}_2^2} + \frac{X_v \rho e^{i\omega}}{\sqrt{X_v^2 - \tilde{y}_2^2}}$$

Consequently, equation (C4) can be evaluated as

$$\lim_{\rho \to 0} \rho \int_{\omega = \omega_1}^{\omega = \omega_1 - 2\pi} \frac{W\left(\tilde{x}, X_v + \rho e^{i\omega}\right) i e^{i\omega}}{X_v + \rho e^{i\omega} - X} \, d\omega$$

$$= \frac{\Gamma_v}{2\pi\left(X_v - X\right)} \lim_{\rho \to 0} \rho \int_{\omega = \omega_1}^{\omega = \omega_1 - 2\pi} \log_e \left(\frac{X_v \rho e^{i\omega}}{\sqrt{X_v^2 - \tilde{y}_2^2}} \right) e^{i\omega} \, d\omega = 0$$

In a similar fashion it can be shown that the last term in equation (C3) vanishes. Consider the fourth and fifth terms in equation (C3). It can be shown that ΔW has the values Γ_v and $-\Gamma_v$ on the feeding sheets from $X\left(S_{max}\right)$ to X_v and $-X^*\left(S_{max}\right)$ to $-X_v^*$, respectively. It follows that

$$\int_{S = X\left(s_{max}\right)}^{S = X_v} \frac{\Delta W(\tilde{x}, S)}{S - X} \, dS = -\Gamma_v \log_e \left[1 - \frac{X_v - X\left(s_{max}\right)}{X_v - X} \right] \qquad \text{(C5)}$$

$$\int_{S=-X^*(s_{max})}^{S=-X_v^*} \frac{\Delta W(\tilde{x},S)}{S - X}\, dS = \Gamma_v \log_e \left[1 - \frac{X_v^* - X^*(s_{max})}{X_v^* + X}\right] \tag{C6}$$

Assume that several turns of the vortex sheet are included as shown in figure 11. From this figure it can be seen that for points X located near the wing surface

$$\left|X_v - X(s_{max})\right| \ll \left|X_v - X\right|$$

$$\left|X_v^* - X^*(s_{max})\right| \ll \left|X_v^* + X\right|$$

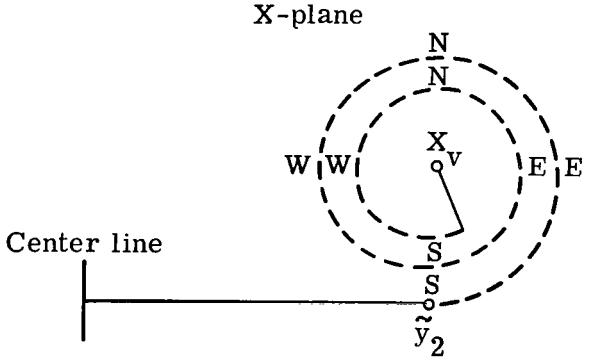

(a) Physical plane.

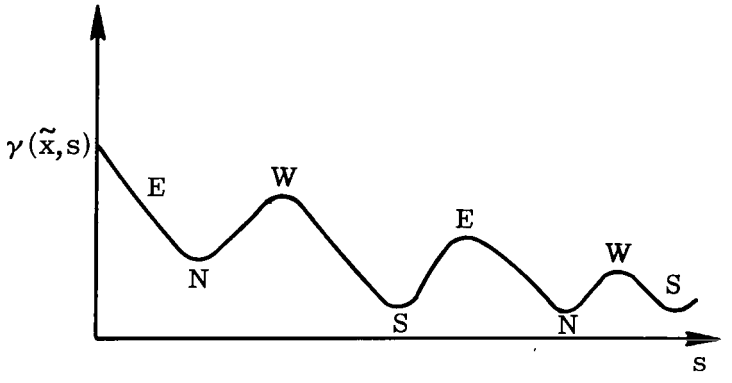

(b) Vortex-sheet strength.

Figure 11.- Variation of vortex-sheet strength.

It follows from these inequalities and equations (C5) and (C6) that

$$\left|\int_{S=X(s_{max})}^{S=X_v} \frac{\Delta W(\tilde{x},S)}{S - X}\, dS\right| + \Gamma_v = \Gamma_v\left|\frac{X_v - X(s_{max})}{X_v - X}\right| + \ldots << 1$$

$$\left|\int_{S=-X^*(s_{max})}^{S=-X_v^*} \frac{\Delta W(\tilde{x},S)}{S - X}\, dS\right| - \Gamma_v = \Gamma_v\left|\frac{X_v^* - X^*(s_{max})}{X_v^* + X}\right| + \ldots << 1$$

It is concluded that the potential ϕ_1 for separated leading-edge flow can be approximated as

$$\phi_1 = \mathrm{Re}\left[\frac{1}{\pi i}\int_{s=-s_{max}}^{s=-\tilde{y}_2} \frac{\gamma(\tilde{x},s)}{X(s) - X}\, ds + \frac{1}{\pi i}\int_{s=-\tilde{y}_2}^{s=\tilde{y}_2} \frac{\gamma(\tilde{x},s)}{S - X}\, ds + \frac{1}{\pi i}\int_{s=\tilde{y}_2}^{s=s_{max}} \frac{\gamma(\tilde{x},s)}{X(s) - X}\, ds\right] \tag{C7}$$

where it is assumed that the flow model includes several turns of the vortex sheet as shown in figure 11.

Consider the derivative ϕ_1'. From equation (C7) it can be shown that

$$\phi_1' = \frac{1}{2\pi i}\left\{\int_{s=-\tilde{y}_2}^{s=\tilde{y}_2} \gamma'(\tilde{x},s)\left(\frac{1}{s - X} - \frac{1}{s - X^*}\right) ds + \gamma(\tilde{x},s_{max})\left[\frac{X'(s_{max})}{X(s_{max}) - X} - \frac{X^{*\prime}(s_{max})}{X^*(s_{max}) - X^*}\right.\right.$$

$$\left.\left. + \frac{X^{*\prime}(s_{max})}{X^*(s_{max}) + X} - \frac{X'(s_{max})}{X(s_{max}) + X^*}\right]\right\} \tag{C8}$$

In the derivation of this equation, the facts that for a symmetric flow field $\gamma(\tilde{x},s)$ is antisymmetric about the wing center line and that the quantity $\gamma'(\tilde{x},s)$ is very small at all points on the vortex sheet have been used. The last condition, which arises because the vortex sheet can support no force, is obtained from equation (20) of reference 18. It is well known that the magnitude of the vortex-sheet strength diminishes as distance along the sheet from the wing tip increases; a schematic of the type of behavior which Smith (ref. 20) found for a delta wing is shown in figure 11. Consequently, the contribution of the nonintegral terms in equation (C8) can be made arbitrarily small by increasing the size of the vortex sheet sufficiently. As a result, equation (C8) is approximated in this appendix as

$$\phi_1'(\tilde{x},X,X^*) = \frac{1}{2\pi i}\int_{s=-\tilde{y}_2}^{s=\tilde{y}_2} \gamma'(\tilde{x},s)\left(\frac{1}{s - X} - \frac{1}{s - X^*}\right)ds \tag{C9}$$

It should be noted that equation (C9) is exact for attached leading-edge flow.

Solution for ϕ_{2a}

This derivation is the same as that of reference 25. The general form of the particular solution is given by equation (43). The derivative $\phi_1'(\tilde{x},X,X^*)$ is given by equation (C9). As stated previously, the Kutta condition applies at the wing leading edge so that to lowest order

$$\gamma'(\tilde{x},\pm\tilde{y}_2) = 0 \tag{C10}$$

Equation (C10) is exact if the flow is attached at the leading edge. From equations (43), (C9), and (C10), the particular solution for ϕ_{2a} can be written as

$$\phi_{2a}^P = -\frac{\gamma + 1}{32\pi}\frac{\partial}{\partial\tilde{x}}\left\{\int_{s=-\tilde{y}_2}^{s=\tilde{y}_2}\gamma'(\tilde{x},s)\,ds\int_{t=-\tilde{y}_2}^{t=\tilde{y}_2}\frac{\gamma'(\tilde{x},t)}{s - t}\,dt\left[X^*\log_e\left(\frac{s - X}{t - X}\right) + X\log_e\left(\frac{s - X^*}{t - X^*}\right)\right]\right.$$

$$\left. - 2\int_{s=-\tilde{y}_2}^{s=\tilde{y}_2}\gamma'(\tilde{x},s)\log_e(s - X)\,ds\int_{t=-\tilde{y}_2}^{t=\tilde{y}_2}\gamma'(\tilde{x},t)\log_e(t - X^*)\,dt\right\} \tag{C11}$$

From equation (C11) it can be shown that the normal derivative of ϕ_{2a}^P at the wing surface is

$$\frac{\partial\phi_{2a}^P(\tilde{x},\tilde{y},\pm 0)}{\partial\tilde{z}} = \mp\frac{\gamma + 1}{4}\frac{\partial}{\partial\tilde{x}}\left[\gamma'(\tilde{x},\tilde{y})\ \text{P.V.}\int_{s=-\tilde{y}_2}^{s=\tilde{y}_2}\gamma'(\tilde{x},s)\left(\frac{\tilde{y}}{s - \tilde{y}} + \log_e|s - \tilde{y}|\right)ds\right] \tag{C12}$$

where the notation P.V. denotes the principal value of the integral.

The potential ϕ_{2a} must satisfy a homogeneous Neumann boundary condition at the wing surface. As a result, the general form of the complementary solution of ϕ_{2a} is given by equation (47). With equation (C12) the potential ϕ_{2a}^C can be written as

$$\phi_{2a}^C = \frac{\gamma + 1}{16\pi}\int_{s=-\tilde{y}_2}^{s=\tilde{y}_2}\frac{\partial}{\partial\tilde{x}}\left[\gamma'(\tilde{x},s)\ \text{P.V.}\int_{t=-\tilde{y}_2}^{t=\tilde{y}_2}\gamma'(\tilde{x},t)\left(\frac{s}{t - s} + \log_e|s - t|\right)dt\right]\log_e\left[(s - X)(s - X^*)\right]ds \tag{C13}$$

At large radial distances $\tilde{r}$ from the configuration, equation (C13) can be written as

$$\phi_{2a}^{C} = \frac{\gamma + 1}{8\pi} \log_e \tilde{r} \int_{s=-\tilde{y}_2}^{s=\tilde{y}_2} \frac{\partial}{\partial \tilde{x}} \left[\gamma'(\tilde{x},s) \text{ P.V.} \int_{t=-\tilde{y}_2}^{t=\tilde{y}_2} \gamma'(\tilde{x},t) \left(\frac{s}{t-s} + \log_e |t-s| \right) dt \right] ds \qquad \text{(C14)}$$

Solution for ϕ_{2b}

The derivation of this solution is the same as that of reference 25. The general form of the particular solution is given by equation (44). The appropriate form of the potential ϕ_1 to be used in evaluating this solution is given by equation (29). It follows from equations (44) and (29) that ϕ_{2b}^{P} near the wing surface and the normal derivative of ϕ_{2b}^{P} at the wing surface are, respectively,

$$\phi_{2b}^{P}(\tilde{x},\tilde{y},\tilde{z}) = \frac{1}{\lambda^2} \left[m_{\pm}'(\tilde{x},\tilde{y}) + g''(\tilde{x},\tilde{y})\,\tilde{z} \right] \left\{ m_{\pm}(\tilde{x},\tilde{y}) - \left[1 - g'(\tilde{x},\tilde{y}) \right] \tilde{z} \right\} \qquad \text{(C15)}$$

and

$$\frac{\partial \phi_{2b}^{P}(\tilde{x},\tilde{y},\pm 0)}{\partial \tilde{z}} = \frac{1}{\lambda^2} \left\{ m_{\pm}(\tilde{x},\tilde{y})\, g''(\tilde{x},\tilde{y}) - m_{\pm}'(\tilde{x},\tilde{y}) \left[1 - g'(\tilde{x},\tilde{y}) \right] \right\} \qquad \text{(C16)}$$

The potential ϕ_{2b} must satisfy a homogeneous Neumann boundary condition at the wing surface. Consequently, the general form of the complementary solution of ϕ_{2b} is

$$\phi_{2b}^{C} = -\frac{1}{8\pi} \int_{s=-\tilde{y}_2}^{s=\tilde{y}_2} \left[\frac{\partial \phi_{2b}^{P}(\tilde{x},s,+0)}{\partial \tilde{z}} - \frac{\partial \phi_{2b}^{P}(\tilde{x},s,-0)}{\partial \tilde{z}} \right] \log_e \left[(s - X)(s - X^*) \right] ds \qquad \text{(C17)}$$

When equation (C16) is substituted into equation (C17), it is found that the complementary solution is

$$\phi_{2b}^{C} = -\frac{1}{4\pi\lambda^2} \int_{s=-\tilde{y}_2}^{s=\tilde{y}_2} \left\{ m(\tilde{x},s)\, g''(\tilde{x},s) - m'(\tilde{x},s) \left[1 - g'(\tilde{x},s) \right] \right\} \log_e \left[(s - X)(s - X^*) \right] ds \qquad \text{(C18)}$$

where the function m is given by equation (49). At large radial distances $\tilde{r}$ from the configuration, equation (C18) can be written as

$$\phi_{2b}^{C} = -\frac{1}{2\pi\lambda^2} \log_e \tilde{r} \int_{s=-\tilde{y}_2}^{s=\tilde{y}_2} \left\{ m(\tilde{x},s)\, g''(\tilde{x},s) - m'(\tilde{x},s) \left[1 - g'(\tilde{x},s) \right] \right\} ds \qquad \text{(C19)}$$

Solution for ϕ_{2c}

The general form of the particular solution for ϕ_{2c} is given by equation (46). With this equation and equation (29) for the potential ϕ_1 near the wing surface, it can be shown that ϕ_{2c}^P near the wing surface and the normal derivative of ϕ_{2c}^P at the wing surface are, respectively,

$$\phi_{2c}^P(\tilde{x},\tilde{y},\tilde{z}) = \frac{\tilde{z}}{\lambda^2}\left\{m_\pm(\tilde{x},\tilde{y}) - \left[1 - g'(\tilde{x},\tilde{y})\right]\tilde{z}\right\} \tag{C20}$$

and

$$\frac{\partial\phi_{2c}^P(\tilde{x},\tilde{y},\pm 0)}{\partial\tilde{z}} = \frac{1}{\lambda^2}\, m_\pm(\tilde{x},\tilde{y}) \tag{C21}$$

The potential ϕ_{2c} must satisfy homogeneous Neumann boundary conditions at the wing surface. Consequently, the general form of the complementary solution of the potential ϕ_{2c} is

$$\phi_{2c}^C = -\frac{1}{8\pi}\int_{s=-\tilde{y}_2}^{s=\tilde{y}_2}\left[\frac{\partial\phi_{2c}^P(\tilde{x},s,+0)}{\partial\tilde{z}} - \frac{\partial\phi_{2c}^P(\tilde{x},s,-0)}{\partial\tilde{z}}\right]\log_e\left[(s - X)(s - X^*)\right] ds \tag{C22}$$

With equation (C21), equation (C22) can be written as

$$\phi_{2c}^C = -\frac{1}{4\pi\lambda^2}\int_{s=-\tilde{y}_2}^{s=\tilde{y}_2} m(\tilde{x},s)\log_e\left[(s - X)(s - X^*)\right] ds \tag{C23}$$

where the function $m(\tilde{x},\tilde{y})$ is given by equation (49). At large radial distances $\tilde{r}$ from the configuration, equation (C23) can be written as

$$\phi_{2c}^C = -\frac{1}{2\pi\lambda^2}\log_e\tilde{r}\int_{s=-\tilde{y}_2}^{s=\tilde{y}_2} m(\tilde{x},s)\, ds \tag{C24}$$

APPENDIX D

THIRD-ORDER INNER POTENTIALS

Consider the third-order terms in inner expansion (eq. (16)). When this expansion is substituted into equation (7) subject to the assumption that α, λ, and ν are related by equation (54), it is found that the potential $\phi_{3,3}$ is governed by the two-dimensional Laplace equation in the cross-flow plane and that the potentials $\phi_{3,2}$ and $\phi_{3,1}$ are governed by the Poisson equations

$$\tilde{\nabla}_2^2 \phi_{3,2} = (\gamma + 1)\left[\phi_1'\left(\frac{1}{a^2}\varphi_{\delta,1}' + \phi_{2,2}'\right)\right]' \tag{D1}$$

$$\tilde{\nabla}_2^2 \phi_{3,1} = -\frac{K^2}{a^2}\phi_1'' + \frac{2}{a^2\lambda^2}\left(\frac{\partial \varphi_\delta'}{\partial \tilde{r}}\sin\theta + \frac{1}{\tilde{r}}\frac{\partial \varphi_\delta'}{\partial \theta}\cos\theta\right) + (\gamma + 1)\left[\phi_1'\left(\frac{1}{a^2}\varphi_\delta' + \phi_{2,1}'\right)\right]'$$

$$+ \frac{2}{\lambda^2}\left(\frac{\partial \phi_1}{\partial \tilde{r}}\frac{\partial \varphi_\delta}{\partial \tilde{r}} + \frac{1}{\tilde{r}^2}\frac{\partial \phi_1}{\partial \theta}\frac{\partial \varphi_\delta}{\partial \theta}\right)' \tag{D2}$$

It is also found that the potential ϕ_3 is governed by a Poisson equation with the same degree of complexity as equation (7). For large values of the inner radial variable $\tilde{r}$, the equation for ϕ_3 can be written as

$$\tilde{\nabla}_2^2 \phi_3 = (\gamma + 1)\left(\phi_1'\phi_2'\right)' + \ldots \tag{D3}$$

The particular solutions to equations (D1), (D2), and (D3) for $\tilde{r} >> \tilde{y}_2$ are

$$\phi_{3,2}^P = -\frac{\gamma + 1}{2}\left\{f'\left[\frac{1}{a^2}\left(F_e F_e'\right)' + \frac{\gamma + 1}{4}\left(f'f''\right)'\right]\right\}' \tilde{r}\log_e \tilde{r}\sin\theta$$

$$\phi_{3,1}^P = \frac{1}{2}\left\{(\gamma + 1)\left[f'\left(\frac{1}{a^2}g_\delta' + g_{2,1}'\right)\right]' - \frac{K^2}{a^2}f'' - \frac{\gamma + 1}{2a^2}\left[f'\left(F_e F_e'\right)'\right]'\right\}\tilde{r}\log_e \tilde{r}\sin\theta$$

$$+ \frac{\gamma + 1}{4a^2}\left[f'\left(F_e F_e'\right)'\right]'\tilde{r}\log_e^2 \tilde{r}\sin\theta$$

$$\phi_3^P = \frac{\gamma+1}{2}\left(\left(f'g_2'\right)' - \frac{1}{2}\left(f'H'\right)' + \frac{\gamma+1}{8}\left[f'\left(f'f''\right)'\right]' + \frac{\gamma+1}{4}\left\{f'\left[f'\left(\frac{1}{\lambda^2} - \frac{\gamma+1}{4}f''\right)\right]'\right\}'\right)$$

$$\times \tilde{r}\log_e \tilde{r}\sin\theta + \frac{\gamma+1}{4}\left\{\left(f'H'\right)' - \frac{\gamma+1}{4}\left[f'\left(f'f''\right)'\right]'\right\}\tilde{r}\log_e^2 \tilde{r}\sin\theta$$

$$+ \frac{(\gamma+1)^2}{24}\left[f'\left(f'f''\right)'\right]'\tilde{r}\log_e^3 \tilde{r}\sin\theta + \ldots$$

It can be seen that if the complementary solutions $\phi_{3,3}^C$ and $\phi_{3,2}^C$ are of the form

$$\phi_{3,3}^C = \frac{\gamma+1}{4}\left\{f'\left[\frac{1}{a^2}\left(F_e F_e'\right)' + \frac{\gamma+1}{3}\left(f'f''\right)'\right]\right\}'\tilde{r}\sin\theta$$

$$\phi_{3,2}^C = \frac{1}{2}\left((\gamma+1)\left\{f'\left[\frac{1}{a^2}g_\delta' + g_{2,1}' - \frac{1}{a^2}\left(F_e F_e'\right)' + \frac{1}{2}H' - \frac{\gamma+1}{8}\left(f'f''\right)'\right]\right\}' - \frac{K^2}{a^2}f''\right)\tilde{r}\sin\theta$$

the sum of the third-order terms in the inner expansion when written in terms of outer variables for large values of the inner radial variable $\tilde{r}$ satisfies the equation

$$\lambda^7 \sin^3\alpha\left[\log_e^3\frac{1}{\lambda\nu}\phi_{3,3} + \log_e^2\frac{1}{\lambda\nu}\phi_{3,2} + \log_e\frac{1}{\lambda\nu}\phi_{3,1} + \phi_3\right] = O\left[\frac{\lambda^6\sin^3\alpha}{\nu}\log_e\frac{1}{\lambda\nu}\right]$$

$$= O\left[\frac{\nu^2}{\sqrt{\log_e\frac{1}{\lambda\nu}}}\right] << \nu^2 = \epsilon_1$$

It is seen that this sum is not of lower order than ϵ_1. The same relationship can be shown to hold for the sums of the fourth and higher order terms of the inner expansion.

REFERENCES

1. Oswatitsch, Klaus; and Keune, Friedrich (K. W. Mangler, transl.): A Theorem of Equivalence for Wings of Small Aspect Ratio at Zero Incidence in Transonic Flow. Lib. Transl. No. 545, Brit. R.A.E., Aug. 1955.

2. Whitcomb, Richard T.: A Study of the Zero-Lift Drag-Rise Characteristics of Wing-Body Combinations Near the Speed of Sound. NACA Rep. 1273, 1956. (Supersedes NACA RM L52H08.)

3. Heaslet, Max A.; and Spreiter, John R.: Three-Dimensional Transonic Flow Theory Applied to Slender Wings and Bodies. NACA Rep. 1318, 1957. (Supersedes NACA TN 3717.)

4. Messiter, Arthur F., Jr.: Expansion Procedures and Similarity Laws for Transonic Flow. AFOSR-TN-57-626, DDC No. AD 136 613, U.S. Air Force, Sept. 1957.

5. Hayes, Wallace D.: La Seconde Approximation Pour les Écoulements Transsoniques non Visqueux. J. Mecan., vol. 5, no. 2, June 1966, pp. 163-206.

6. Lifshits, Yu. B.: Transonic Flow Past Slender Bodies. NASA TT F-13,251, 1970.

7. Cheng, H. K.; and Hafez, Mohammed: Three-Dimensional Structure and Equivalence Rule of Transonic Flows. AIAA J., vol. 10, no. 8, Aug. 1972, pp. 1115-1117.

8. Barnwell, R. W.: Transonic Flow About Lifting Configurations. AIAA J., vol. 11, no. 5, May 1973, pp. 764-766.

9. Cheng, H. K.; and Hafez, M. M.: Equivalence Rule and Transonic Flow Theory Involving Lift. AIAA J., vol. 11, no. 8, Aug. 1973, pp. 1210-1212.

10. Liepmann, H. W.; and Roshko, A.: Elements of Gasdynamics. John Wiley & Sons, Inc., c.1957.

11. Cole, Julian D.; and Messiter, Arthur F.: Expansion Procedures and Similarity Laws for Transonic Flow. Part 1. Slender Bodies at Zero Incidence. Z. Angew. Math. Phys., vol. VIII, fasc. 1, 1957, pp. 1-25.

12. Kaplun, Saul; and Lagerstrom, P. A.: Asymptotic Expansions of Navier-Stokes Solutions for Small Reynolds Numbers. J. Math. Mech., vol. 6, no. 5, Sept. 1957, pp. 585-593.

13. Van Dyke, Milton: Perturbation Methods in Fluid Mechanics. Academic Press, Inc., 1964.

14. Sneddon, Ian N.: Elements of Partial Differential Equations. McGraw-Hill Book Co., Inc., 1957.

15. Spreiter, John R.: The Aerodynamic Forces on Slender Plane- and Cruciform-Wing and Body Combinations. NACA Rep. 962, 1950. (Supersedes NACA TN's 1897 and 1662.)

16. Ward, G. N.: Supersonic Flow Past Slender Pointed Bodies. Quart. J. Mech. Appl. Math., vol. II, pt. 1, Mar. 1949, pp. 75-97.

17. Jones, Robert T.: Properties of Low-Aspect-Ratio Pointed Wings at Speeds Below and Above the Speed of Sound. NACA Rep. 835, 1946. (Supersedes NACA TN 1032.)

18. Wei, M. H. Y.; Levinsky, E. S.; and Su, F. Y.: Nonconical Theory of Flow Past Slender Wing-Bodies With Leading-Edge Separation. NASA CR 73446, [1969].

19. Mangler, K. W.; and Smith, J. H. B.: A Theory of Flow Past a Slender Delta Wing With Leading Edge Separation. Proc. Roy. Soc. (London), ser. A, vol. 251, no. 1265, May 26, 1959, pp. 200-217.

20. Smith, J. H. B.: Improved Calculations of Leading-Edge Separation From Slender Delta Wings. Tech. Rep. No. 66070, Brit. R.A.E., Mar. 1966.

21. Mirels, Harold: Aerodynamics of Slender Wings and Wing-Body Combinations Having Swept Trailing Edges. NACA TN 3105, 1954.

22. Mangler, K. W.: Calculation of the Pressure Distribution Over a Wing at Sonic Speeds. R. & M. No. 2888, Brit. A.R.C., 1955.

23. Klunker, E. B.; and Harder, Keith C.: General Solutions for Flow Past Slender Cambered Wings With Swept Trailing Edges and Calculation of Additional Loading Due to Control Surfaces. NACA TN 4242, 1958.

24. Stocker, P. M.: Supersonic Flow Past Bodies of Revolution With Thin Wings of Small Aspect Ratio. Aeronaut. Quart., vol. III, pt. I, May 1951, pp. 61-79.

25. Cheng, H. K.; and Hafez, M. M.: Equivalence Rule and Transonic Flows Involving Lift. USCAE 124, Univ. of Southern California, Apr. 1973.

26. Ashley, Holt; and Landahl, Marten: Aerodynamics of Wings and Bodies. Addison-Wesley Pub. Co., Inc., c.1965.

27. Spreiter, John R.; and Alksne, Alberta Y.: Slender-Body Theory Based on Approximate Solution of the Transonic Flow Equation. NASA TR R-2, 1959.

28. Aoyama, Kinya; and Wu, Jain-Ming: On Transonic Flow Field Around Tangent Ogive Bodies. AIAA Paper No. 70-189, Jan. 1970.

29. Bailey, Frank R.: Numerical Calculation of Transonic Flow About Slender Bodies of Revolution. NASA TN D-6582, 1971.

30. Murman, Earll M.; and Cole, Julian D.: Calculation of Plane Steady Transonic Flows. AIAA J., vol. 9, no. 1, Jan. 1971, pp. 114-121.

31. Lomax, Harvard; Bailey, Frank R.; and Ballhaus, William F.: On the Numerical Simulation of Three-Dimensional Transonic Flow With Application to the C-141 Wing. NASA TN D-6933, 1973.

32. Barnwell, R. W.: Transonic Flow About Lifting Wing-Body Combinations. AIAA Paper No. 74-185, Jan.-Feb. 1974.

33. Brown, Clinton E.; and Michael, William H., Jr.: On Slender Delta Wings With Leading-Edge Separation. NACA TN 3430, 1955.

"The aeronautical and space activities of the United States shall be conducted so as to contribute . . . to the expansion of human knowledge of phenomena in the atmosphere and space. The Administration shall provide for the widest practicable and appropriate dissemination of information concerning its activities and the results thereof."

—NATIONAL AERONAUTICS AND SPACE ACT OF 1958

NASA SCIENTIFIC AND TECHNICAL PUBLICATIONS

TECHNICAL REPORTS: Scientific and technical information considered important, complete, and a lasting contribution to existing knowledge.

TECHNICAL NOTES: Information less broad in scope but nevertheless of importance as a contribution to existing knowledge.

TECHNICAL MEMORANDUMS: Information receiving limited distribution because of preliminary data, security classification, or other reasons. Also includes conference proceedings with either limited or unlimited distribution.

CONTRACTOR REPORTS: Scientific and technical information generated under a NASA contract or grant and considered an important contribution to existing knowledge.

TECHNICAL TRANSLATIONS: Information published in a foreign language considered to merit NASA distribution in English.

SPECIAL PUBLICATIONS: Information derived from or of value to NASA activities. Publications include final reports of major projects, monographs, data compilations, handbooks, sourcebooks, and special bibliographies.

TECHNOLOGY UTILIZATION PUBLICATIONS: Information on technology used by NASA that may be of particular interest in commercial and other non-aerospace applications. Publications include Tech Briefs, Technology Utilization Reports and Technology Surveys.

Details on the availability of these publications may be obtained from:

SCIENTIFIC AND TECHNICAL INFORMATION OFFICE

NATIONAL AERONAUTICS AND SPACE ADMINISTRATION

Washington, D.C. 20546